On Blind Channel Estimation in Full-duplex Wireless Relay Systems

Konstantin Muranov, Besma Smida, *Senior Member, IEEE,* and Natasha Devroye, *Senior Member, IEEE*

***Abstract*—We investigate the feasibility of second-order statistics-based blind channel estimation in the context of two-hop full-duplex relay systems. To that end, the performance of blind and traditional pilot-based (training sequence based) channel estimation approaches are compared. This is accomplished by deriving the Cramer-Rao Lower Bound (CRLB) expressions for both blind and pilot-based schemes, and comparing them to each other and to the mean-squared error (MSE) values measured via simulation. Post-equalization SINR expressions are also derived for both blind and pilot-based methods. Furthermore, a modified post-equalization SINR expression, where the channel estimation error is replaced by the inverse of the Fisher information matrix (FIM) is proposed, providing an upper bound for the post-equalization SINR. These analytically-predicted SINR values for the blind approach are compared to the SINR measured via link simulation. The performance of the two channel estimation methods is analyzed by comparing the CRLB, post-equalization SINR, and BER performance for two significantly different transmission packet sizes. All of the above metrics indicate that blind estimation provides clear performance advantages relative to the pilot-based counterpart. Additionally, the blind approach eliminates the overhead associated with the pilot-based method, where a portion of the system resources is allocated to the pilot sequence. To quantify this, the spectral efficiency of the FD relay system employing blind and pilot-based channel estimation methods are compared, indicating that at high SNR, the blind approach provides around 2-bps/Hz spectral efficiency gain relative to a typical pilot-based method. Finally, the computational complexity of the two channel estimation techniques are evaluated and compared. The blind approach has a clear computational advantage for larger packet sizes.**

***Index Terms*—Wireless relay, full-duplex, blind channel estimation, channel equalization.**

I. Introduction

A. Motivation

WIRELESS relay systems can improve network coverage and data rates at the expense of a moderate increase in system complexity. The transmitter and receiver of a half-duplex (HD) node employ orthogonal channels to avoid interfering with one another. This orthogonality is achieved by utilizing different frequencies, time slots, or orthogonal spread-spectrum codes. In contrast, the transmitter and receiver of a full-duplex (FD) system operate on the same channel, which can significantly improve spectral efficiency. For this reason and due to the recent advances [8], [15], FD transceivers are increasingly being considered. One such application is full-duplex wireless relaying. Fig. 1 shows a two-hop FD relaying system where the source-relay and relay-destination radio links use the same frequency channel at the same time. In contrast to HD relays, FD relay nodes may be seamlessly inserted between the source and destination with minimum impact on the system configuration while improving the signal coverage.

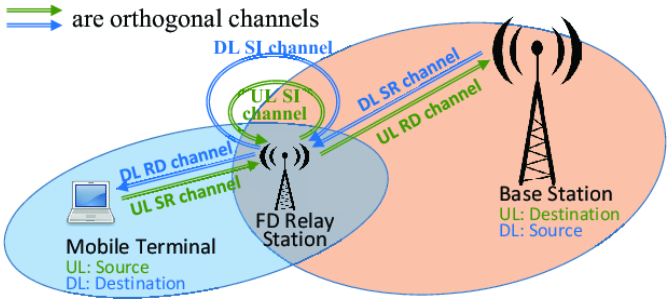

Fig. 1. High-level view of a two-hop full-duplex relay system.

B. Related Work

The feasibility of using full-duplex relaying was initially studied in [23] and [21], where the end-to-end capacity expressions were derived for amplify-and-forward (AF) and decode-and-forward (DF) full-duplex relay systems. It was shown that FD relay schemes provided end-to-end channel capacity improvement relative to their HD counterparts when residual SI levels were below certain *break-even* levels. Furthermore, it was found that the break-even levels vary depending on the relative gains of the source-relay (SR) and relay-destination (RD) channels as well as the power levels at the source and relay transmitters. Since then, a number of SI mitigation techniques were proposed, particularly in the context of full-duplex relaying. The spatial SI suppression in MIMO-based full-duplex AF relaying and the impact of the SI channel estimation errors were considered in [17], where it was shown that methods that suppress SI while maximizing SIR at the relay transmitter and receiver provide better channel capacity performance than zero-forcing methods focusing only on SI suppression. The combination of time-domain cancellation and spatial suppression techniques such as null-space projection, antenna and beam selection were evaluated in [22]. It was concluded that these techniques provide sufficient SI mitigation and that FD relay systems can ensure reliable communications.

The use of blind channel estimation has the potential to further improve the spectral efficiency. Hence, it is of interest to evaluate the feasibility of its use in the context of the FD

Konstantin Muranov, Besma Smida, Natasha Devroye are with the Department of Electrical and Computer Engineering, University of Illinois at Chicago, e-mail: kmuran2@uic.edu, smida@uic.edu, devroye@uic.edu. The work of B. Smida was partially supported by NSF award 1620902. The work of N. Devroye was partially supported by NSF under award 1815428. The contents of this article are solely the responsibility of the authors and do not necessarily represent the official views of the NSF.

relay system. The main advantage of blind channel estimation is that it eliminates the need for a training sequence. In practical wireless communication protocols, pilot-sequence-based training uses a non-negligible portion of the overall radio resource budget. However, the potential spectral efficiency improvement resulting from freeing up the resources occupied by the pilot sequence comes at the expense of an increased receiver complexity. In this work, we consider the sub-space-based blind channel estimation approach proposed in [18]. It takes advantage of the cyclostationary properties of the oversampled or multi-antenna signals. It belongs to a class of blind estimation techniques relying on the second-order statistics, which require fewer data samples than the higher-order statistics-based methods. Consequently, this method can be used for time-varying channels.

Unlike [13], where the system did not involve a relay link, and blind channel estimation in the context of a point-to-point FD system was considered in terms of joint estimation of SI and other channels, here we investigate the use of blind channel estimation at various stages of the FD relay link independently of the SI channel estimation. Since the signal transmitted by the relay node is mostly known to the relay transceiver, blind estimation of the SI channel is typically not necessary. In contrast to [13], we consider the system-wide effects of blind channel estimation at both the relay and destination on the end-to-end performance. Finally, in [13], the phase-ambiguity issue inherent to blind estimation based on the second-order statistics (SOS) was addressed using an interesting approach based on non-symmetric constellations, while this work relies on differentially-encoded modulation in combination with an K-th power phase recovery technique.

C. Contributions

We study the feasibility of blind channel estimation in the context of a two-hop FD relay system. This is accomplished by analyzing and comparing the performance of blind and pilot-based estimators.

1) Analytical CRLB and post-equalization SINR expressions: We derive the analytical CRLB expressions for the blind and pilot-based channel estimators. The CRLB expression for the blind channel estimation provides an interesting insight into the channel estimation behavior at the destination of the relay link considered here. Specifically, the expression predicts that blind estimation performance at the destination is independent of the SINR level at the relay receiver. As shown in Fig. 3a, this analytical prediction is confirmed by the behavior of the blind channel estimation NMSE measured at the destination of the uplink relay configuration. To the best of our knowledge, the CRLB of the blind channel estimation has not been derived for the FD relay configurations considered here.

Next, an analytical expression for the post-equalization SINR at the destination of the two-hop FD relay link is derived. An upper bound expression for the SINR is proposed by incorporating the effect of channel estimation error in the form of the inverse Fisher Information Matrix (FIM) of the channel estimator. In contrast to directly using the estimation error, the proposed FIM-based SINR expression allows for a purely analytical computation of the post-equalization SINR. This provides an alternative to the link simulation or physical system prototyping that would be necessary in order to measure actual estimation error directly from link simulation or physical system prototyping. The post-equalization SINR is an important performance metric that can be used for computing the spectral efficiency of a communication link, and this type of analytical post-equalization SINR expression has not been proposed in prior work (neither for FD relay system, nor for a general point-to-point link). The CRLB and post-equalization SINR computed using these analytical expressions are then compared to the NMSE and post-equalization SINR measured from the link simulation.

2) Feasibility study of blind channel estimation: The feasibility of employing the sub-space-based blind channel estimation in the context of FD relay system is further analyzed by comparing several performance metrics for the blind and pilot-based estimation approaches. These metrics include BER at the destination receiver, CRLB of the channel estimation error, the analytically predicted upper bound for post-equalization SINR, as well as the actual post-equalization SINR measured at the destination receiver via simulation. We also evaluate the sensitivity of the system performance to the transmission burst size, i.e., to the number of received samples that can be used for channel estimation. To this end, the system performance is compared for smaller and larger packet lengths, where the packet size determines the number of symbols available for computing the channel estimate. The practicality of the blind channel estimation is considered by evaluating the system performance under different residual self-interference levels and non-linear effects inherent in FD transceivers. Furthermore, the computational complexity of the blind and pilot-based methods is compared.

3) Two channel equalization configurations: In our preliminary work in [19], we compared the performance of two FD relay link configurations: a) *distributed channel equalization*, where in addition to SI mitigation, the SR channel equalization is performed at the relay, while RD channel equalization is performed at the destination; b) *end-point channel equalization*, where only SI mitigation and signal amplification are performed at the relay, while channel equalization is performed only at the destination node. Here we focus primarily on the distributed configuration, in part, because it was shown in [19] that under ideal channel estimation conditions, the distributed approach provides much better performance. Also, as shown in Fig. 2, the *end-point* configuration does not allow the use of the SIMO model for the relay-destination link. Hence, for the remainder of this text, the reader should assume that the discussion pertains to the distributed configuration, unless indicated otherwise. For the purpose of completeness, we include performance results for the end-point configuration assuming sub-channel orthogonality, without making assumptions regarding specific sub-channel multiplexing methods at the relay transmitter. Both analytical and simulation results show that the distributed configuration results in better channel estimation performance, post-equalization SINR, and BER at the destination. All of these advantages are attributed to

the diversity combining (of multiple sub-channels) during the channel equalization at the relay. Furthermore, simulation results indicate better resilience of the distributed configuration to the non-linearities present in the SI signal.

4) FIR approximation: The presence of the self-interference feedback loop in a FD system results in an IIR relay equivalent model. However, we show that a robust discrete-time cancellation of the residual self-interference allows one to approximate the relay model as an FIR system. Specifically, the performance of the residual SI cancellation technique described in [19] satisfies this requirement. Adopting the same SI cancellation method, we show that the FD relay system is able to achieve the same BER performance as the corresponding HD relay link (Fig. 5a). This confirms that the post-cancellation SI level is negligibly small, and that our FIR approximation is appropriate. The Linear Least Square Error (LLSE) estimation of the SI channel described in [19] achieves the CRLB under the linear channel conditions. We will demonstrate that this method performs almost as well for non-linear SI channel (Fig. 5b).

5) Spectral efficiency comparison between blind and pilot-based channel estimation: Finally, the spectral efficiency of the blind FD approach is compared to a pilot-based method, as well as to a HD system. Results indicate that at high SNR, the proposed blind approach provides 2 bps/Hz spectral efficiency gain relative to the pilot-based approach. This is the case for both longer and shorter transmission bursts. The simulation results indicate that blind channel estimation is able to achieve BER performance that is very close to that of the pilot-based estimation (even considering different pilot allocation ratios), while at the same time using far fewer resources.

TABLE I
NOTATION SUMMARY

notation	description of the quantity
$\mathbf{s}_{s;n}$	signal vector transmitted by the source node
$\mathbf{s}_{r;n}$	signal vector transmitted by the relay node
$\mathbf{S}_{s;n}$	filtering matrix for source Tx signal, $\mathbf{s}_{s;n}$
$\mathbf{S}_{r;n}$	filtering matrix for relay Tx signal, $\mathbf{s}_{r;n}$
$\mathbf{h}_{sr;n}^{(i)}$	source-relay (SR) sub-channel i, instance n
$\mathbf{h}_{rd;n}^{(i)}$	relay-destination (RD) sub-channel i, instance n
$\mathbf{h}_{rr;n}^{(i)}$	self-interference (SI) sub-channel i, instance n
$\mathbf{H}_{sr;n}$	SR channel filtering matrix
$\mathbf{H}_{rr;n}$	SI channel filtering matrix
$\mathbf{H}_{rd;n}$	RD channel filtering matrix
$\mathbf{H}_{sd;n}$	source-destination (SD) filtering matrix - End-point: $\mathbf{H}_{sd;n}=\mathbf{H}_{rd;n}\mathbf{H}_{sr;n}$ - Distributed: $\mathbf{H}_{sd;n}=\mathbf{H}_{rd;n}\mathbf{F}_{r;n}\mathbf{H}_{sr;n}$
$\mathbf{w}_{r;n}$	complex AWGN at the relay receiver, $\mathbf{w}_{r;n}\sim\mathcal{CN}(\mathbf{0},\sigma_1^2\mathbf{I})$
$\mathbf{w}_{d;n}$	complex AWGN at the destination receiver, $\mathbf{w}_{d;n}\sim\mathcal{CN}(\mathbf{0},\sigma_2^2\mathbf{I})$
$\mathbf{x}_{sr;n}$	signal at the output of SR channel: $\mathbf{H}_{sr;n}\mathbf{s}_{s;n}$
$\mathbf{x}_{rr;n}$	signal at the output of SI channel: $\mathbf{H}_{rr;n}\mathbf{s}_{r;n}$
$\mathbf{x}_{rd;n}$	signal at the output of RD channel: $\mathbf{H}_{rd;n}\mathbf{s}_{r;n}$
$\mathbf{F}_{r;n}$	relay equalizer filtering matrix
$\mathbf{F}_{d;n}$	destination equalizer filtering matrix
$\mathbf{y}_{r;n}$	combined RX signal and noise at the relay
$\mathbf{y}_{d;n}$	combined RX signal and noise at destination
$\mathbf{C}_{y;\,n}^{K}$	covariance matrix of the received signal Ex: at the destination, $\mathbf{C}_{y;\,n}^{K}=E\left[\mathbf{y}_{d;\,n}^{K}(\mathbf{y}_{d;\,n}^{K})^{H}\right]$
$\mathbf{C}_{sy;\,n}^{K}$	cross-covariance matrix of the transmitted and received signal. Ex: $\mathbf{C}_{sy;\,n}^{K}=E\left[\mathbf{s}_{s;\,n}^{K}(\mathbf{y}_{d;\,n}^{K})^{H}\right]$
K	dimensionality of covariance matrices ($K<<A$)
M	channel order
L	number of sub-channels (oversampling rate)
A	number of signal samples for which channel realization stays the same ($A>>M$)
p	processing delay within the relay transceiver, measured in symbol intervals

II. SYSTEM MODEL AND NOTATION

A. Notation

In the remainder of the text, vectors and matrices are represented by bold lower-case and upper-case letters, respectively. The first part of the subscript signifies the signal or channel type, e.g., s, r, d correspond to the source, relay, and destination, respectively. The second part of the subscript represents the index, e.g., n. For signal vectors, this is the index of the first element within the vector. For channel vectors, the index corresponds to the channel realization corresponding to the packet, where the first symbol has index n. Unless otherwise specified, the vectors are assumed to have length A. For example, a vector starting at the sampling index n and representing the additive noise sequences at the relay receiver is denoted as $\mathbf{w}_{r;n}=\left[w_r[n],\ldots,w_r[n+A-1]\right]^T$. We will represent an estimate of a quantity by adding the "hat", and estimation error - by adding "tilde". For example, the estimate and the estimation error of the self-interference channel matrix are denoted by $\widehat{\mathbf{H}}_{rr;n}$ and $\widetilde{\mathbf{H}}_{rr;n}$, respectively, where $\widetilde{\mathbf{H}}_{rr;\,n}=\mathbf{H}_{rr;\,n}-\widehat{\mathbf{H}}_{rr;\,n}$.

B. Two-hop FD Relay Channel Model

In this section we define the system model and describe relevant assumptions. The FD relay system considered here is depicted in Fig. 2, where it is assumed that there is no direct link from the source to the destination. The blind channel estimation process considered in this paper requires presence of a Single-In-Multiple-Out (SIMO) channel, composed of L sub-channels. According to [18], the desired SIMO configuration can be achieved either by sampling the received signal at L times the symbol rate or by using L sensors, e.g., spatially-separated receive antennas. Either approach is applicable to the relay link configuration. Without loss of generality, we assume that the oversampling approach is employed, where each of L sampling phases represents a sub-channel within a SIMO model. For sampling phase $i=0,...,L-1$, the signal at the relay receiver is defined as

$$\mathbf{y}_{r;n}^{(i)}=\mathbf{S}_{s;\,n}\mathbf{h}_{sr;\,n}^{(i)}+\mathbf{S}_{r;\,n}\mathbf{h}_{rr;\,n}^{(i)}+\mathbf{w}_{r;\,n}^{(i)}=$$
$$=\mathbf{H}_{sr;\,n}^{(i)}\mathbf{s}_{s;\,n}+\mathbf{H}_{rr;\,n}^{(i)}\mathbf{s}_{r;\,n}+\mathbf{w}_{r;\,n}^{(i)}. \quad (1)$$

The signal at the destination node receiver is given by

$$\mathbf{y}_{d;\,n}^{(i)}=\mathbf{x}_{rd;\,n}^{(i)}+\mathbf{w}_{d;\,n}^{(i)}=\mathbf{S}_{r;\,n}\mathbf{h}_{rd;\,n}^{(i)}+\mathbf{w}_{d;\,n}^{(i)}=$$
$$=\mathbf{H}_{rd;\,n}^{(i)}\mathbf{s}_{r;\,n}+\mathbf{w}_{d;\,n}^{(i)}. \quad (2)$$

The simplified single sub-channel model of FD relay is derived in *Appendix* A. Furthermore, we assume that all propagation channels in (1) and (2) are frequency-selective with finite impulse response of order M. As a result, the structure and dimensions of the matrices $\mathbf{S}_{s;\,n}\mathbf{h}_{sr;\,n}^{(i)}$, $\mathbf{S}_{r;\,n}\mathbf{h}_{rr;\,n}^{(i)}$, and

$\mathbf{S}_{s;\,n}\mathbf{h}^{(i)}_{sr;\,n}$ are the same. We assume frequency-selective fading channels with delay spread equal to T_d symbol intervals. The duration of the transmission packet is assumed to be within the coherence time, T_c, of the channel, as justified by [31], where it is argued that the coherence time T_c of wireless channels is significantly greater (by an order of 10^3) than the delay spread T_d. The realizations of the sub-channel impulse responses are assumed to be statistically independent from each other. Also, we assume that AWGN components are statistically-independent for each sub-channel. The output of the i^{th} SR sub-channel is given by the discrete-time convolution of the $[A\times 1]$ transmitted signal vector, $\mathbf{s}_{s;n}$, and the sampled impulse response of the SR channel, $\mathbf{h}^{(i)}_{sr;\,n}$, of order M. Depending on the context, we will use one of the two equivalent representations of such convolution operation, $\mathbf{H}^{(i)}_{sr;\,n}\mathbf{s}_{s;\,n} = \mathbf{S}_{s;\,n}\mathbf{h}^{(i)}_{sr;\,n}$, where $\mathbf{H}^{(i)}_{sr;\,n} = \left[\mathbf{h}^{(i)}_{sr;\,(n,0)},\, ...,\, \mathbf{h}^{(i)}_{sr;\,(n,A-1)}\right]$ and $\mathbf{S}_{s;\,n} = \left[\mathbf{s}_{s;\,(n,0)},\, ...,\, \mathbf{s}_{s;\,(n,M)}\right]$ are $[A\times A]$ and $[A\times(M+1)]$ filtering matrices, respectively. In the case of $\mathbf{H}^{(i)}_{sr;\,n}$, each column has at most $M+1$ non-zero elements:

$$\left[\mathbf{h}^{(i)}_{sr;\,(n,0)}, \mathbf{h}^{(i)}_{sr;\,(n,1)}, ..., \mathbf{h}^{(i)}_{sr;\,(n,A-1)}\right] =$$

$$= \begin{bmatrix} h^{(i)}_{sr;\,n}[0] & 0 & ... & 0 \\ h^{(i)}_{sr;\,n}[1] & h^{(i)}_{sr;\,n}[0] & ... & 0 \\ h^{(i)}_{sr;\,n}[2] & h^{(i)}_{sr;\,n}[1] & ... & 0 \\ \vdots & \vdots & & \vdots \\ 0 & 0 & ... & h^{(i)}_{sr;\,n}[0] \end{bmatrix}. \quad (3)$$

The columns of $\mathbf{S}_{s;\,n}$ are defined as,

$$\left[\mathbf{s}_{s;\,(n,0)}, \mathbf{s}_{s;\,(n,1)}, ..., \mathbf{s}_{s;\,(n,M)}\right] =$$

$$= \begin{bmatrix} s_s[n] & 0 & ... & 0 \\ s_s[n+1] & s_s[n] & ... & 0 \\ s_s[n+2] & s_s[n+1] & ... & 0 \\ \vdots & \vdots & & \vdots \\ s_s[n+A-1] & s_s[n+A-2] & ... & s_s[n+A-M] \end{bmatrix}. \quad (4)$$

The system equation (1) is valid for both *end-point* and *distributed* configurations. As seen in Fig. 2, the difference between the two configurations is manifested in the definition of the signal, $\mathbf{s}_{r;\,n}$ and is due to the presence of SR channel equalization in the distributed case,

$$\text{End-point: } \mathbf{s}_{r;\,n}{=}\hat{\mathbf{x}}_{sr;\,n}, \quad \text{Distributed: } \mathbf{s}_{r;\,n}{=}\mathbf{F}_{r;\,n}\hat{\mathbf{x}}_{sr;\,n}, \quad (5)$$

where $\mathbf{F}_{r;\,n}$ is the relay equalizer filtering matrix, and $\hat{\mathbf{x}}_{sr;\,n}$ is the post-SI-cancellation signal at the relay:

$$\hat{\mathbf{x}}_{sr;\,n} = \mathbf{H}_{sr;\,n-p}\,\mathbf{s}_{n-p} + \mathbf{w}_{r;\,n-p} + \widetilde{\mathbf{H}}_{rr;\,n}\,\mathbf{s}_{r;\,n-2p}. \quad (6)$$

In the distributed approach, the SI cancellation is followed by channel equalization, while in the end-point configuration, the SI cancellation is also performed, but the signal is transmitted by the relay node without channel equalization. It is assumed that decoding is only performed at the destination. Therefore, once the channel equalization is performed at the relay, the symbols are not mapped back to the specific constellation points. Unlike the method described in [27], the log likelihood ratio values are not computed either. Instead, the processed samples are passed directly to the relay transmitter (Fig. 2). The block z^{-p} models the relay processing delay of p symbol intervals. The non-linearities and amplification gains at the relay transmitter are discussed in the next section.

C. SI model

It is assumed that self-interference is reduced to a manageable level by antenna separation [26], [2] and analog cancellation techniques [7], [20], [25], [12]. The residual SI is then estimated and canceled digitally. The estimation of the SI channel at the relay is impaired not only by AWGN, but also by interference from the SR signal, $\mathbf{x}_{sr;\,n} = \mathbf{S}_{r;\,n}\mathbf{h}_{sr;\,n}$. In practical full-duplex systems, some amount of noise and non-linear distortion is present at both transmitter and receiver, [24], [25], [33], [1], [14], [10]. We assume that at least a portion of the non-linear distortion is mitigated via analog methods leaving some residual non-linear distortion. Performance of the system is examined for different levels of this residual non-linear distortion, using the model described in [14]. According to this model, the signal $\mathbf{s}_{r;\,n}$ transmitted by the relay is affected by the non-linearity and becomes

$$\breve{\mathbf{s}}_{r;\,n} = \alpha_s\mathbf{s}_{r;\,n} + \eta_4\eta_3\eta_2 \begin{bmatrix} s^*_r[n] \\ s^*_r[n{+}1] \\ s^*_r[n{+}2] \\ \vdots \\ s^*_r[n{+}A{-}1] \end{bmatrix} + \eta_5(\eta_3\eta_1)^3 \begin{bmatrix} |s_r[n]|^2 s_r[n] \\ |s_r[n{+}1]|^2 s_r[[n{+}1] \\ |s_r[n{+}2]|^2 s_r[n{+}2] \\ \vdots \\ |s_r[n{+}A{-}1]|^2 s_r[n{+}A{-}1] \end{bmatrix}, \quad (7)$$

for some scalars $\eta_1, \eta_2, ..., \eta_5 \in R$ that are described next. Since the non-linear effects present at the transmitter are much more dominant than those present at the receiver, we ignore the non-linearities at the receiver side. The first term in (7) represents the linear portion of the transmitted signal with relative gain $\alpha_s = \eta_4\eta_3\eta_1$. The second term in (7) corresponds to the image of the signal, and the third term represents the non-linearity introduced in the power amplifier (PA). We define δ as the ratio between the primary signal component to the third-order component as $\delta = 20\log_{10}\left(\frac{\eta_4\eta_3\eta_1}{\eta_5(\eta_3\eta_1)^3}\right)$. η_1 and η_2 are relative gains of the main signal and image signal components, respectively, and are related to each other via Image Rejection Ration, IRR $= \eta_1/\eta_2$. The gain of the Variable Gain Amplifier (VGA) is $\eta_3 = \text{VGA}_{gain}$. η_4 is a relative gain of the linear component at the output of PA, and η_5 is a gain of the third-order term at the output of PA. These two gains are related via the IIP3 parameter as IIP3 $= \sqrt{\eta_4/\eta_5}$. Similarly to [14], we use following set of parameters resulting in $\delta = 20dB$: IRR $= 25$dB, IIP3 $=$ 20dB, $\text{VGA}_{gain} = 10$dB, $\text{PA}_{gain} = 27$dB.

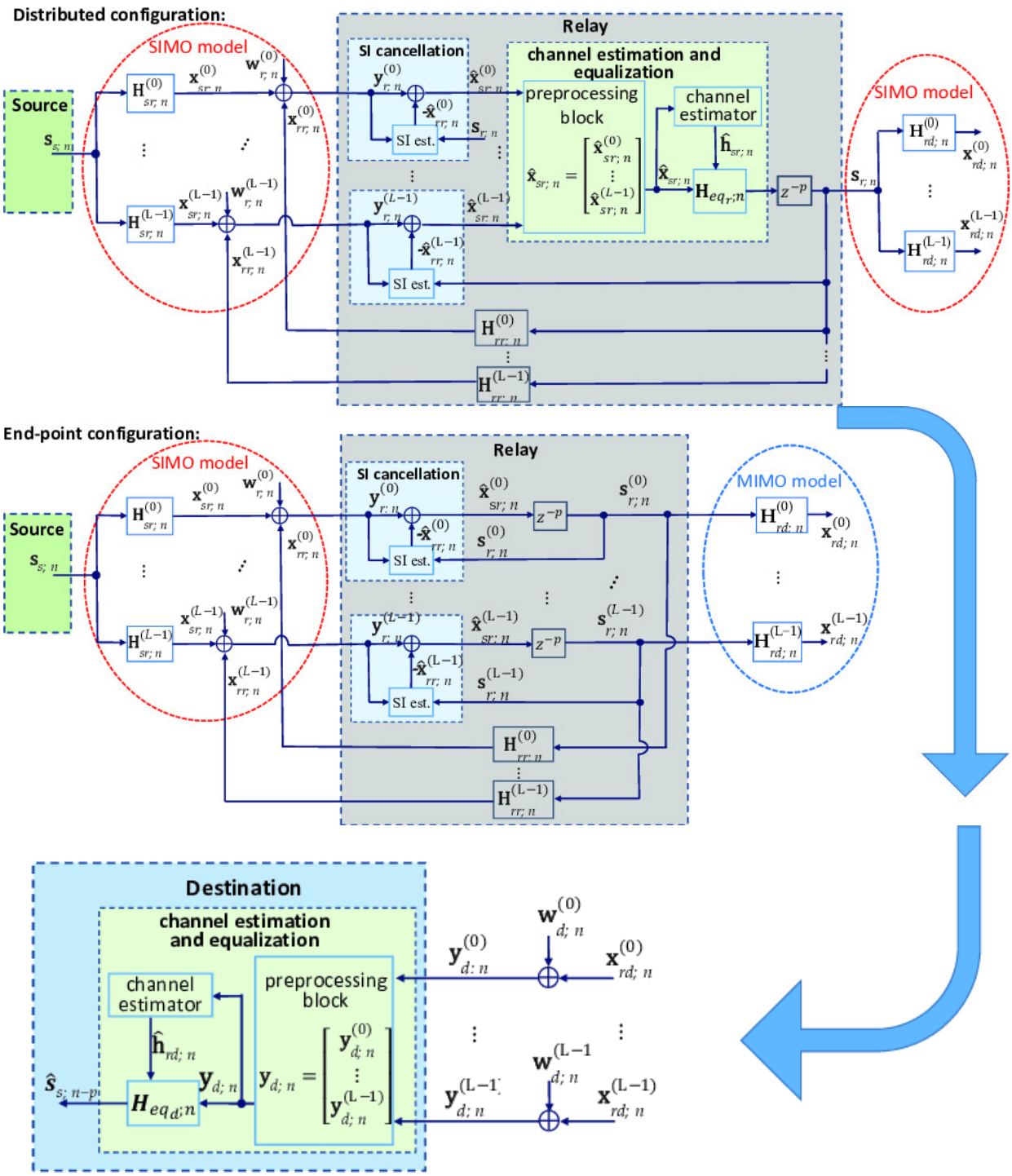

Fig. 2. Simplified full-duplex relay system: Distributed and End-point configurations

III. Channel Estimation and Equalization

A. Blind Channel Estimation

In addition to evaluating the performance of the end-point and distributed equalization, our goal is to study the feasibility of employing blind channel estimation in a two-hop relay link. To that end, we will derive the Cramer-Rao Lower Bound (CRLB) of the channel estimation error variance at the destination node of the relay link. We then derive the expression (20) for the post-equalization SINR at the destination of this FD relay system. This expression is then modified by incorporating the FIM in order to provide analytical tight upper bound for the post-equalization SINR given in (21). In this section, we provide a brief description of the blind estimation method used and the associated multi-channel notation. Initially proposed in [18], this method is based on [29] and [28], but exploits the *eigenstructure* of the received signal covariance matrix more efficiently, resulting in reduced computational complexity. According to [32], this class of methods performs worse than optimal moment-based estimation techniques. However, it was selected due to its

TABLE II
NOTATION FOR EXPRESSION (8)

channel estimate at:	notation:
relay (distributed)	$\mathbf{y}_{z_1}$=$\mathbf{y}_r$, $\mathbf{H}_{z_2}$=$\mathbf{H}_{sr}$, $\mathbf{s}_{z_3}$=$\mathbf{s}_s$, $\mathbf{w}_{z_4}$=$\mathbf{w}_r$.
destination (end-point)	$\mathbf{y}_{z_1}$=$\mathbf{y}_d$, $\mathbf{H}_{z_2}$=$\mathbf{H}_{sd}$, $\mathbf{s}_{z_3}$=$\mathbf{s}_s$, $\mathbf{w}_{z_4}$=$\mathbf{w}_{eff}$.
destination (distributed)	$\mathbf{y}_{z_1}$=$\mathbf{y}_d$, $\mathbf{H}_{z_2}$=$\mathbf{H}_{rd}$, $\mathbf{s}_{z_3}$=$\mathbf{s}_r$, $\mathbf{w}_{z_4}$=$\mathbf{w}_{eff}$.

simplicity and robustness when the identifiability constraints described in [18] are met. This method takes advantage of cyclostationarity by oversampling of the received analog signal by integer factor $L > 1$ of the symbol rate. The signals corresponding to each of L sampling phases are treated as though they passed through L parallel sub-channels. In the relay link of Fig. 2, the channel estimation is performed at the relay and destination nodes based on the signals defined in (6) and (2), respectively, each yielding different blind channel estimation performance. In the interest of conciseness, we describe the blind channel estimation for a simplified generic system, where the different sampling instances of the received signal can be combined into one expression as follows,

$$\begin{bmatrix} \mathbf{y}_{z_1;\,n}^{(0)} \\ \vdots \\ \mathbf{y}_{z_1;\,n}^{(L-1)} \end{bmatrix} = \begin{bmatrix} \mathbf{H}_{z_2}^{(0)} \\ \vdots \\ \mathbf{H}_{z_2}^{(L-1)} \end{bmatrix} \mathbf{s}_{z_3;\,n} + \begin{bmatrix} \mathbf{w}_{z_4;\,n}^{(0)} \\ \vdots \\ \mathbf{w}_{z_4;\,n}^{(L-1)} \end{bmatrix}$$

$$\text{or equivalently,} \quad \mathbf{Y}_{z_1;\,n} = \mathbf{H}_{z_2}\mathbf{s}_{z_3;\,n} + \mathbf{W}_{z_4;\,n}, \qquad (8)$$

and the vectors, $\mathbf{y}_{z_1;\,n}^{(i)}, \mathbf{s}_{z_3;\,n}, \mathbf{w}_{z_4;\,n}^{(i)}$, represent $(N{+}M)$-sample segments of the A-sample received signal, transmitted signal, and noise vectors, respectively. In this notation, M is the channel impulse response order, and N is the evaluation interval satisfying $N \geq M$ and $(N+M) << A$. As outlined in Table II, the subscripts in expression (8) take on different meanings depending on the configuration (end-point vs. distributed), as well as the location where the channel estimation is performed (relay vs. destination).

This type of channel estimation requires that there are no common zeros among the sub-channels, [34], [28]. For the end-point configuration, this implies that the signals corresponding to different sub-channels remain independent as they pass through the relay and transmitted by the relay to the destination. Hence, in contrast to the SIMO channel in the case of *distributed* equalization, the RD channel is a MIMO channel for the *end-point* case. The equivalent model block diagrams of Fig. 2 depict the differences between the two configurations. This outline of the blind channel estimation approach assumes that $\mathbf{w}_{z_4;\,n}^{(i)}$ is AWGN. However, due to propagation of the relay noise and residual self-interference to the destination receiver, $\mathbf{w}_{z_4;\,n}^{(i)}$ is correlated, resulting in sub-optimal performance. However, we will show later that even under these conditions, the distributed method with blind channel estimation provides sufficient improvement in spectral efficiency over the pilot-based schemes. The $LN \times LN$ covariance matrix of the zero-mean oversampled input vector $\mathbf{Y}_{z_1;\,n}$ is given by

$$\mathbf{C}_y = E\big(\mathbf{Y}_{z_1;\,n}\mathbf{Y}_{z_1;\,n}^H\big) = \mathbf{H}_{z_2}\mathbf{C}_s\mathbf{H}_{z_2}^H + \mathbf{C}_w = \\ = \sum_{k=0}^{N+M-1} \lambda_k \mathbf{q}_k\mathbf{q}_k^H + \sigma_w^2 \sum_{j=0}^{LN-N-M-1} \mathbf{g}_j\mathbf{g}_j^H, \qquad (9)$$

where the last step is based on the spectral theorem, λ_k, $\mathbf{q}_k$ are the eigenvalues and eigenvectors associated with the signal sub-space, σ_w^2, $\mathbf{g}_j$ are the eigenvalues and eigenvectors associated with the noise sub-space of $\mathbf{C}_y$. As proposed in [18], the channel can be estimated by minimization of the quadratic form:

$$\Phi(\mathbf{h}_{z_2}) = \sum_{k=0}^{LN-N-M-1} \|\mathbf{g}_k^H\mathbf{H}_{z_2}\|^2 = \sum_{k=0}^{LN-N-M-1} \mathbf{g}_k^H\mathbf{H}_{z_2}\mathbf{H}_{z_2}^H\mathbf{g}_k. \qquad (10)$$

Since the eigenvector scaled by a complex scalar is also an eigenvector for the same matrix, this second-order-statistics-based blind estimation scheme suffers from scaling factor ambiguity. [13] resolved this issue by introducing an asymmetric constellation. In contrast, we address it by employing the differentially-encoded modulation.

B. Pilot-based Channel Estimation

An MMSE approach is assumed for pilot-based channel estimation. The pilot symbols are updated at the relay transmitter with the same ideal pilot sequence as that transmitted by the source. Specifically, the following expression is used for estimating the i^{th} sub-channel at the relay and then at the destination receivers:

$$\widehat{\mathbf{h}}_{z_2;\,n}^{(i)} = \left(\mathbf{C}_{hh,z_1}^{(i)}\right)^{-1}\mathbf{S}_p^H\left(\mathbf{C}_{y,z_1}^{(i)}\right)^{-1}\mathbf{y}_{pilot;\,n}^{(i)} = \\ = \mathbf{C}_{y,z_1}^{(i)}\mathbf{S}_p^H\left[\mathbf{S}_p\mathbf{C}_{y,z_1}^{(i)}\mathbf{S}_p^H\right]^{-1}\mathbf{y}_{pilot;\,n}^{(i)}, \qquad (11)$$

where $i = 0, ..., L-1$ and the $(M+1)\times(M+1)$ covariance matrix is $\mathbf{C}_{y,z_1}^{(i)} = \mathbf{S}_p\mathbf{h}_{z_2;\,n}^{(i)}\left(\mathbf{h}_{z_2;\,n}^{(i)}\right)^H\mathbf{S}_p^H + \mathbf{C}_{w_d}^{(i)}$. According to [11], it can be shown that the FIM and CRLB for the distributed case are:

$$\text{FIM: } \mathbf{J}(\mathbf{h}_{rd;\,n}) = \mathbf{S}_{p;\,n-p}^H\mathbf{C}_{w_d}^{-1}\mathbf{S}_{p;\,n-p},$$

$$\text{CRLB}(\mathbf{h}_{rd;\,n}) = \left(\mathbf{S}_p^H\mathbf{C}_{w_d}^{-1}\mathbf{S}_p\right)^{-1}. \qquad (12)$$

C. SI estimation

We can consider $\mathbf{x}_{sr;\,n}$ and $\mathbf{w}_{r;\,n}$ in (1) to be impairments to the estimation of the SI signal. If we assume that the magnitude of $\mathbf{x}_{sr;\,n}$ follows a Rayleigh PDF, this would imply that these samples have complex Gaussian PDF with zero mean. Hence, $\mathbf{w}_{rr;\,n} = \mathbf{x}_{sr;\,n} + \mathbf{w}_{r;\,n}$ is a sum of two independent complex Gaussian-distributed random vectors with different means and autocorrelation matrices (in both, end-point and distributed configurations):

$$\mathbf{x}_{sr;\,n} = \mathbf{H}_{sr;\,n}\mathbf{s}_{s;\,n} \sim \mathcal{CN}(\mathbf{0}, \mathbf{C}_{sr}), \;\; \mathbf{w}_{r;\,n} \sim \mathcal{CN}(\mathbf{0}, \mathbf{I}\sigma_{w_r}^2). \qquad (13)$$

Hence, the effective noise vector, $\mathbf{w}_{rr;\,n} = (\mathbf{H}_{sr;\,n}\mathbf{s}_{s;\,n} + \mathbf{w}_{r;\,n})$, is also Gaussian [30], $\mathbf{w}_{rr;\,n} \sim \mathcal{CN}(\mathbf{0}, \mathbf{C}_{w_{rr}})$. Considering equation (1) in light of the above assumptions, we have $\mathbf{y}_{r;\,n} \sim \mathcal{CN}(\mu_{y_r}, \mathbf{C}_{y_r})$, where $\mu_{y_r} = \mathbf{S}_{r;\,n}\mathbf{h}_{rr;\,n} = \mathbf{S}_{r;\,n}\gamma_{rr}\widetilde{\mathbf{h}}_{rr;\,n}$, and covariance matrices are $\mathbf{C}_{y_r} = \varepsilon_s\mathbf{H}_{sr;\,n}\mathbf{H}_{sr;\,n}^H + \mathbf{I}\sigma_{w_r}^2$. The residual SI channel

estimation is assumed to be based on Linear Least Squares Estimator (LLSE):

$$\widehat{\mathbf{h}}_{rr;\,n} = \left(\mathbf{S}_{r;\,n}^H \mathbf{C}_{y_r}^{-1} \mathbf{S}_{r;\,n}\right)^{-1} \mathbf{S}_{r;\,n}^H \mathbf{C}_{y_r}^{-1} \mathbf{y}_{r;\,n}, \tag{14}$$

where $\mathbf{y}_{r;\,n}$ is the signal received at the relay (1), $\mathbf{S}_{r;\,n}$ is the filtering matrix composed of the samples transmitted by the relay. The inclusion of covariance matrix $\mathbf{C}_{y_r}$ is due to the fact that estimation is performed in the presence of non-white complex Gaussian noise, $\mathbf{w}_{eff;\,n}$, consisting of the output of the SR channel and relay receiver noise. Under these conditions, the estimator given by expression (14) is considered to be efficient [11]. The estimated SI channel and the samples transmitted by the relay are used for generating an estimate of the SI signal as $\widehat{\mathbf{x}}_{rr;\,n} = \mathbf{S}_{r;\,n} \widehat{\mathbf{h}}_{rr;\,n}$, which is then subtracted from the total received signal as shown in Fig.2.

D. Channel equalization

Fig. 2 depicts the *distributed* and *end-point* equalization approaches. It is possible to estimate the SI and SR channels jointly at the relay. However, in order to facilitate comparison between the two configurations, we assume that in the distributed case, SI estimation and cancellation is performed first, followed by SR channel equalization. One of our goals is to analyze the impact of the presence of the channel equalization at the relay on the end-to-end BER performance in the context of blind channel estimation. The equalizer expressions are discussed next.

Distributed: The expression for the MMSE equalizer at the relay receiver is given by

$$\mathbf{F}_{r;\,n} = \mathbf{C}_{sy_r;\,n} \mathbf{C}_{y_r;\,n}^{-1} = \mathbf{H}_{sr;\,n}^H \left[\mathbf{H}_{sr;\,n} \mathbf{H}_{sr;\,n}^H + \mathbf{C}_{w_r;\,n}\right]^{-1}, \tag{15}$$

where $\mathbf{C}_{w_r;\,n} = \widetilde{\mathbf{H}}_{rr;\,n} \mathbf{F}_{r;\,n-p} \mathbf{H}_{sr;\,n-p} \mathbf{H}_{sr;\,n-p}^H \mathbf{F}_{r;\,n-p}^H \widetilde{\mathbf{H}}_{rr;\,n}^H + \sigma_r^2 \left(\widetilde{\mathbf{H}}_{rr;\,n} \mathbf{F}_{r;\,n-p} \mathbf{F}_{r;\,n-p}^H \widetilde{\mathbf{H}}_{rr;\,n}^H + \mathbf{I}\right)$. The MMSE channel equalizer expression at the destination receiver is derived in *Appendix B*:

$$\mathbf{F}_{d;\,n} = \mathbf{C}_{s_r y;\,n} \mathbf{C}_{y;\,n}^{-1} \approx \mathbf{C}_{s_r y;\,n} \mathbf{C}_{y;\,n}^{-1} =$$

$$= \mathbf{H}_{rd;\,n}^H \mathbf{C}_{y;\,n}^{-1} = \mathbf{H}_{rd;\,n}^H \left(\mathbf{H}_{rd;\,n} \mathbf{H}_{rd;\,n}^H + \mathbf{C}_{w_{eff1};\,n}\right)^{-1}, \tag{16}$$

where the noise covariance matrix is defined as,

$$\mathbf{C}_{w_{eff1};\,n} \approx$$

$$\mathbf{H}_{eff1;\,n} \mathbf{F}_{r;\,n-p} \mathbf{H}_{sr;\,n-2p} \mathbf{H}_{sr;\,n-2p}^H \mathbf{F}_{r;\,n-p}^H \mathbf{H}_{eff1;\,n}^H + \frac{1}{\mathrm{SNR}_r} \mathbf{H}_{rd;\,n} \mathbf{F}_{r;\,n} \left(\widetilde{\mathbf{H}}_{rr;\,n} \widetilde{\mathbf{H}}_{rr;\,n}^H + \mathbf{I}\right) \mathbf{F}_{r;\,n}^H \mathbf{H}_{rd;\,n}^H + \frac{1}{\mathrm{SNR}_d} \mathbf{I}. \tag{17}$$

In the above derivation, it is assumed that the blind approach is not able to estimate the source-to-destination channel, $\mathbf{H}_{sd;\,n}$. Instead, the relay-destination channel, $\mathbf{H}_{rd;\,n}$, is estimated at the destination. This assumption is due to the presence of the equalizer, $\mathbf{F}_{r;\,n}$, at the relay. At high SNR levels, this results in the all-pass channel, $\mathbf{F}_{r;\,n} \mathbf{H}_{sr;\,n-p}$ with zeros located around the unit circle, which according to [34], [28], does not satisfy the identifiability condition for the second-order-statistics-based blind channel estimation. In order to reduce the number of variables in comparing the blind vs. pilot-based approaches, we propose that $\mathbf{H}_{rd;\,n}$ is estimated at the destination for the pilot-based approach as well. This is facilitated by "refreshing" the pilot symbols at the relay, i.e., replacing the received pilot symbols by the ideal pilot sequence identical to that transmitted by the source. Hence, we propose the use of the following equalizer at the destination (for both blind and pilot-based approaches),

$$\mathbf{F}_{d;\,n} = \mathbf{C}_{sy;\,n} \mathbf{C}_{y;\,n}^{-1} \approx \mathbf{C}_{s_r y;\,n} \mathbf{C}_{y;\,n}^{-1} = \mathbf{H}_{rd;\,n}^H \mathbf{C}_{y;\,n}^{-1}$$

$$\approx \mathbf{H}_{rd;\,n}^H \left(\mathbf{H}_{rd;\,n} \mathbf{H}_{rd;\,n}^H + \mathbf{C}_{w_{eff1};\,n}\right)^{-1}. \tag{18}$$

End-point: The derivation of the destination receiver MMSE channel equalizer for the *end-point* configuration is provided in *Appendix C*. The resulting expression is as follows:

$$\mathbf{F}_{d;\,n} = \mathbf{C}_{sy;\,n} \mathbf{C}_{y;\,n}^{-1} = \mathbf{H}_{sd;\,n}^H \left[\mathbf{H}_{sd;\,n} \mathbf{H}_{sd;\,n}^H + \mathbf{C}_{w_{eff2};\,n}\right]^{-1}, \tag{19}$$

where $\mathbf{H}_{sd;\,n} = \mathbf{H}_{rd;\,n} \mathbf{H}_{sr;\,n}$, $\mathbf{H}_{eff2;\,n} = \mathbf{H}_{rd;\,n} \widetilde{\mathbf{H}}_{rr;\,n} \mathbf{H}_{sr;\,n-2p}$,

$$\mathbf{C}_{w_{eff_2};\,n} \approx \mathbf{H}_{eff2;\,n} \mathbf{H}_{eff2;\,n}^H + \sigma_{w_r}^2 \mathbf{H}_{rd;\,n} \left(\widetilde{\mathbf{H}}_{rr;\,n} \widetilde{\mathbf{H}}_{rr;\,n}^H + \mathbf{I}\right) \mathbf{H}_{rd;\,n}^H + \sigma_{w_d}^2 \mathbf{I}.$$

E. Expression for post-equalization SINR at the destination of the FD relay link

The expression for post-equalization SINR is derived in *Appendix D*. It incorporates both channel estimation error at the destination and the SI cancellation error at the relay.

Distributed Equalization: The expression (21) for upper bound on post-equalization SINR can then be obtained by replacing the channel estimation error covariance matrix, $\widetilde{\mathbf{H}}_{rd;\,n} \widetilde{\mathbf{H}}_{rd;\,n}^H$, by the inverse of FIM, $\mathbf{J}^{-1}(\mathbf{h}_{rd;\,n})$. In contrast to (20), where $\widetilde{\mathbf{H}}_{rd;\,n}$ has to be measured, the upper bound expression (21) provides a purely analytical method of predicting the post-equalization SINR performance. The residual SI is incorporated in the covariance matrix expression as shown in equation (22), where assuming robust SI channel estimation, the third term may be neglected.

End-Point Equalization: The expressions for end-point configuration can be obtained from (20) and (21) by replacing $\mathbf{H}_{rd;\,n}$ by $\mathbf{H}_{sd;\,n}$ and assuming the covariance matrix definition given in (23).

F. CRLB for blind channel estimation at the destination of relay link

The CRLB expression for blind channel estimation at the destination of the relay link using distributed equalization is derived in *Appendix E* and is given in (24), where $\mathbf{S}_{r;\,n}$ represents the signal transmitted by the relay defined in (25). In (25), the noise and residual SI at the relay are included in the signal transmitted by the relay and are not part of the noise covariance matrix. Because these signals pass through the RD channel, they carry the information about this channel. Hence, *blind channel estimation performance at the destination of FD relay using distributed configuration is expected to be independent of the SINR at the relay*.

$$\text{SINR}_{distributed} = \frac{1}{1+\frac{1}{N}\text{tr}\left\{\widetilde{\mathbf{H}}_{rd;\,n}\widetilde{\mathbf{H}}^H_{rd;\,n}\mathbf{C}^{-1}_{y;\,n}\right\}-\frac{1}{N}\text{tr}\left\{\mathbf{H}_{rd;\,n}\mathbf{H}^H_{rd;\,n}\mathbf{C}^{-1}_{y;\,n}\right\}}-1. \tag{20}$$

$$\text{SINR}_{distributed} \leq \frac{1}{1+\frac{1}{N}\text{tr}\left\{\mathbf{J}^{-1}(\mathbf{h}_{rd;\,n})\mathbf{C}^{-1}_{y;\,n}\right\}-\frac{1}{N}\text{tr}\left\{\mathbf{H}_{rd;\,n}\mathbf{H}^H_{rd;\,n}\mathbf{C}^{-1}_{y;\,n}\right\}}-1. \tag{21}$$

Distributed equalization:

$$\begin{aligned}\mathbf{C}_{y;\,n} &= \mathbf{H}_{sd;\,n}\mathbf{H}^H_{sd;\,n}+\mathbf{H}_{rd;\,n}\mathbf{F}_{r;\,n}\widetilde{\mathbf{H}}_{rr;\,n}\mathbf{H}_{sr;\,n-2p}\mathbf{H}^H_{sr;\,n-2p}\widetilde{\mathbf{H}}^H_{rr;\,n}\mathbf{F}^H_{r;\,n}\mathbf{H}^H_{sr;\,n-p}+\mathbf{H}_{rd;\,n}\mathbf{F}_{r;\,n}\widetilde{\mathbf{H}}_{rr;\,n}\widetilde{\mathbf{H}}_{rr;\,n-p}\\ &\quad \mathbf{C}_{s_r;\,n-2p}\widetilde{\mathbf{H}}^H_{rr;\,n-p}\widetilde{\mathbf{H}}^H_{rr;\,n}\mathbf{F}^H_{r;\,n}\mathbf{H}^H_{rd;\,n}+\sigma^2_{w_r}\mathbf{H}_{rd;\,n}\mathbf{F}_{r;\,n}\big(\widetilde{\mathbf{H}}_{rr;\,n}\widetilde{\mathbf{H}}^H_{rr;\,n}+\mathbf{I}\big)\mathbf{F}^H_{r;\,n}\mathbf{H}^H_{rd;\,n}+\sigma^2_{w_d}\mathbf{I},\end{aligned} \tag{22}$$

End-point equalization:

$$\begin{aligned}\mathbf{C}_{y;\,n} &= \mathbf{H}_{sd;\,n}\mathbf{H}^H_{sd;\,n}+\mathbf{H}_{rd;\,n}\widetilde{\mathbf{H}}_{rr;\,n}\mathbf{H}_{sr;\,n-2p}\mathbf{H}^H_{sr;\,n-2p}\widetilde{\mathbf{H}}^H_{rr;\,n}\mathbf{H}^H_{sr;\,n-p}+\mathbf{H}_{rd;\,n}\widetilde{\mathbf{H}}_{rr;\,n}\widetilde{\mathbf{H}}_{rr;\,n-p}\\ &\quad \mathbf{C}_{s_r;\,n-2p}\widetilde{\mathbf{H}}^H_{rr;\,n-p}\widetilde{\mathbf{H}}^H_{rr;\,n}\mathbf{H}^H_{rd;\,n}+\sigma^2_{w_r}\mathbf{H}_{rd;\,n}\big(\widetilde{\mathbf{H}}_{rr;\,n}\widetilde{\mathbf{H}}^H_{rr;\,n}+\mathbf{I}\big)\mathbf{H}^H_{rd;\,n}+\sigma^2_{w_d}\mathbf{I}.\end{aligned} \tag{23}$$

$$\text{CRLB}(\mathbf{h}_{rd;\,n}) = \left[\mathbf{S}^H_{r;\,n}\left(\mathbf{C}^{-1}_{w_{eff}}-\mathbf{C}^{-1}_{w_{eff}}\mathbf{H}_{rd;\,n}\left(\mathbf{H}^H_{rd;\,n}\mathbf{C}^{-1}_{w_{eff}}\mathbf{H}_{rd;\,n}\right)^{-1}\mathbf{H}^H_{rd;\,n}\mathbf{C}^{-1}_{w_{eff}}\right)\mathbf{S}_{r;\,n}\right]^{-1}, \tag{24}$$

$$\mathbf{S}_{r;\,n} = \mathbf{F}_{r;\,n}\mathbf{H}_{sr;\,n}\mathbf{S}_{s;\,n}+\mathbf{F}_{r;\,n}\widetilde{\mathbf{H}}_{rr;\,n}\mathbf{S}_{r;\,n-p}+\mathbf{F}_{r;\,n}\mathbf{w}_{r;\,n}, \quad \text{and} \quad \mathbf{C}_{w_{eff}}=\sigma^2_{w_d}\mathbf{I}. \tag{25}$$

G. Post-equalization SINR measurement via simulation

We now discuss the methodology used for measuring the post-equalization SINR via simulation. At the destination (when equalization is not performed at the relay):

$$\begin{aligned}\hat{s}_s[n] &= \mathbf{f}^H_{d;\,n}\mathbf{h}_{sd;\,n}s[n]+\mathbf{h}^H_{eq_d;\,n}\mathbf{w}_{eff;\,n}=ae^{-j\theta}s_s[n]+\\ &+ae^{-j\theta}\sum_{k=1}^{M}h_{res}[k]s_s[n-k]+ae^{-j\theta}\mathbf{h}^H_{eq_d;\,n}\mathbf{w}_{eff;\,n},\end{aligned} \tag{26}$$

where the first term corresponds to the desired symbol, the second term to the residual ISI, and the third term to post-equalization noise. The scaling factor $ae^{-j\theta}$ is attributed to the scaling factor ambiguity inherent to the blind channel estimation at the destination. Defining,

$$\begin{aligned}R_{\hat{s}s}(0) &= E\left(\hat{s}_s[n]s^*_s[n]\right)=ae^{-j\theta}E\left(|s_s[n]|^2\right)+\\ &+ae^{-j\theta}E\left(\mathbf{h}^H_{eq_d;\,n}\mathbf{w}_{eff;\,n}s^*_s[n]\right)=ae^{-j\theta}\varepsilon_s,\end{aligned} \tag{27}$$

where ε_s is the transmitted symbol energy, and for distributed equalization $\mathbf{w}_{eff;\,n}=\mathbf{H}_{rd;\,n}\mathbf{F}_{r;\,n}\mathbf{w}_{r;\,n}+\mathbf{w}_{d;\,n}$, while for end-point equalization, $\mathbf{w}_{eff;\,n}=\mathbf{H}_{rd;\,n}\mathbf{w}_{r;\,n}+\mathbf{w}_{d;\,n}$. The post-equalization noise variance is then estimated using (28), which represents the actual method for estimation of the post-equalization noise variance directly from the data. Using (27) and (28) we obtain (29).

IV. Simulation Results and Discussion

A. Simulation configuration and performance criteria

As shown in Fig. 1, a base station is assumed at one end of the relay link and a mobile terminal at the other end. The direction from the base station to the mobile is defined as down link (DL), while the reverse direction is up link (UL). A high quality line-of-sight (LOS) link between the relay and base station is assumed, while the link quality between the mobile terminal and the relay can vary significantly. In this section, we will discuss the analytical and simulation results for both UL and DL directions. We focus on the use case, where data is transmitted in bursts (packets) with relatively large periods of silence in between. Since the channel characteristics can significantly change during such transmission gaps, we are mainly concerned with the reliability of the initial channel acquisition, without any kind of cross-packet processing (e.g., filtering). It is also assumed that antenna beam forming and/or the analog SI mitigation techniques described in [4], [5], and [16] are applied at the relay such that only residual self-interference remains. According to [5], such analog SI mitigation techniques can result in residual signal to self-interference ratio (SIR) of 15-25dB. In this section we will examine the end-to-end system performance at slightly more pessimistic 10-dB SIR level. Since larger number of samples allows for more reliable estimation of the second order stationary statistics, it is clear that performance of the blind channel estimation is expected to improve with an increasing number of samples used for computing a single channel estimate. This is true as long as the duration of the transmission packet is less than the coherence time, T_c, of the channel. Therefore, we will examine the channel estimation as well as the overall performance for: $A=280, 1120$ samples that represent small and large packet sizes. These two values of A were selected such that the second value is quadruple of the first in order to cover wide range of the packet sizes. The non-power of 2 values were selected on purpose in order to ensure generality

$$\hat{\sigma}_e^2 = \frac{1}{A}\sum_{n=0}^{A-1}\left|\hat{s}_s[n] - R_{\hat{s}s}(0)\cdot s_s[n]\right|^2 = a^2\frac{1}{A}\sum_{n=0}^{A-1}\left|\sum_{k=1}^{M} h_{res}[k]s_s[n-k] + \mathbf{h}_{eq_d;\,n}^H\mathbf{w}_{eff;\,n}\right|^2, \quad (28)$$

$$\widehat{\text{SINR}}_{sim} = \frac{|R_{\hat{s}s}(0)|^2}{\hat{\sigma}_e^2} = \frac{\varepsilon_s}{\frac{1}{A}\sum_{n=0}^{A-1}\left|\sum_{k=1}^{M} h_{res}[k]s_s[n-k] + \mathbf{h}_{eq_d;\,n}^H\mathbf{w}_{eff;\,n}\right|^2}. \quad (29)$$

of the results. A statistically-independent random realization of the frequency-selective channel is generated every packet duration.

As indicated in the prior paragraphs, in the case of DL most of the signal quality variation is expected to occur at the destination receiver, while in UL direction, poor signal conditions are much more likely to occur at the relay receiver. Hence, DL performance evaluation is conducted by sweeping SNR_d at the destination, while SNR_r at the relay is fixed at 20dB. In the case of UL, the SNR sweep is performed at the relay receiver. The CRLB expressions (24), (25) for the blind channel estimation derived in *Appendix E* predict that blind estimation performance at the destination is impacted by the SNR level at the destination receiver but is independent of the SINR level at the relay receiver. In this section we confirm these analytical predictions by measuring the normalized mean square error (NMSE) of the blind channel estimation at the destination of the UL simulation. Fig. 4a shows that both blind CRLB and NMSE undergo only minor variation as the SINR at the relay receiver is swept from 0dB to 30dB. The reason for this is that both the noise and SI components of the signal received by the relay also pass through the relay-destination channel, and thus enhance the blind channel estimation performance at the destination rather then degrading it. This is why these terms are treated in (24) and (25) as parts of the useful signal transmitted by the relay, rather than as noise and interference at the destination. The situation is quite different for DL direction, where SNR sweep is performed at the destination receiver. In this case, CRLB expressoins (24), (25) predict significant change in the channel estimation NMSE as a function of SNR_d. The NMSE plots of Fig. 3a confirm this prediction.

Furthermore, we evaluate the feasibility of using blind channel estimation by comparing its performance to that of the pilot-based approach. To that end we consider end-to-end BER performance, channel estimation NMSE and CRLB, computational complexity and spectral efficiency. This comparison is repeated for large and small packet sizes as well as for both transmission directions, i.e., DL and UL.

B. Computational Complexity Analysis

The computational complexity of the expression depends on the dimensions of the matrices and vectors involved. The number of floating-point operations (FLOPs) for some common types of matrix transformations (i.e., inversion, eigendecomposition, etc.) were provided in [9], where FLOPs were measured in terms of the combined number of complex multiplications and additions. However, since complex multiplication requires greater number of real arithmetic operations than complex addition, treating these two operations as being equivalent in terms of complexity could lead to wrong conclusions. Instead, we define the FLOP as a real addition or multiplication. Specifically, a complex multiplication requires 4 real multiplications and 2 real additions, while complex addition requires only 2 real additions.

1) Computational Complexity of the Pilot-based Channel Estimator: The computational complexity of the expression (11) depends on the dimensions of the matrices and vectors involved. The following expression provides the computational cost of the MMSE estimator based on expression (11) and was obtained by examining the computational cost of each matrix operation within that expression. *Pilot-based estimation cost*: $L\Big[12(M+1)^2N_p - 4(M+1)N_p + 4(M+1)^3 + 8(M+1)^2 - (M+1) + 4N_p^3 + 16N_p^2 - N_p + 8(M+1)N_p^2\Big]$, where N_p is the number of pilot symbols per packet, M is the channel order, and L is the number of sub-channels.

2) Computational Complexity of the Blind Channel Estimator: The main arithmetic functions needed for blind channel estimation are two eigen decompositions: of covariance matrix $\mathbf{C}_y \in C^{LN\times LN}$ and product matrix $\mathbf{Q} \in C^{L(M+1)\times L(M+1)}$ of the filtering matrices based on the subset of the eigenvectors of $\mathbf{C}_y$. According to [3], the QR-based eigen decomposition of matrix $\mathbf{A} \in C^{n\times n}$ requires $4\times 9n^3$ FLOPs. Hence, the total *computational cost of the blind estimation method:* $36L^3\left[N^3 + (M+1)^3\right]$ FLOPs, where N is the evaluation interval defined in sub-section III-A, M is the channel order, and L is the number of sub-channels.

3) Computational Complexity Comparison: Table III provides computational cost comparison for the pilot-based and blind estimation methods under specific channel order and transmission burst length assumptions used in this paper. The results indicate that computational complexity of the eigen decomposition portion of the blind estimator is independent of the transmission burst size. This results in the blind estimator having greater computational cost than pilot-based approach for short transmission bursts. However, the situation is reversed for larger transmission bursts.

C. Channel Estimation Performance

Fig. 3a and 4a contain channel estimation NMSE and CRLB plots for DL and UL, respectively. These plots facilitate

TABLE III
COMPUTATIONAL COMPLEXITY COMPARISON

channel estimation method	Number of FLOPs (burst size: 280)	Number of FLOPs (burst size: 1120)
pilot-based estimation, 20% pilot alloc.	3.453×10^6	1.896×10^8
blind estimation	4.129×10^6	4.129×10^6

the performance comparison between blind and pilot-based channel estimators. The comparison is performed for small and large data packets. Under the pilot-based approach, 20% of symbols are allocated to the pilot symbols. Both figures indicate that blind channel estimation outperforms the pilot-based approach, both in terms of theoretically achievable performance, i.e., CLRB, as well as the measured NMSE. This is mainly due to the blind approach using every received symbol to compute the estimate instead of just 20% of symbols in the pilot-based approach. According to Fig. 3a, the pilot-based approach is able to achieve the CRLB at the lower and medium SNR levels. However, it falls short of the CRLB at high SNR, where the noise is no longer the main limiting factor, and the imperfections in estimation of the received signal covariance matrix have greater impact on performance. We observed similar results with different pilot/data ratio. There is a significant and constant gap between the measured NMSE and the CRLB for blind estimation. This is not a surprise, as the sub-space-based blind estimation approach is known to be sub-optimal in the MSE sense ([6]). It was mainly selected for its low computational complexity.

As shown in Fig. 4a, the CRLB and NMSE are flat in the case of UL pilot-based estimation since the pilot sequence is refreshed at the relay, so the change in SINR level at the relay receiver has no effect on the channel estimation performance at the destination. The curves corresponding to the blind approach, are also flat but for an entirely different reason. According to (24) and (25), the noise and residual SI at the relay receiver, pass through the relay-destination channel in the same way as the signal of interest. Hence, even the terms corresponding to noise and SI introduced at the relay carry information about the relay-destination propagation channel once they reach the destination. As a result, the blind channel estimation performance at the destination is independent of the SINR_r at the relay. This is an interesting insight that was analytically predicted by the CRLB expression and corroborated by the measured NMSE for blind estimation (Fig. 4a). BER performance comparison between blind and pilot-based channel estimation is captured in Fig. 5a and 5b for DL and UL, respectively. Both figures indicate that blind approach outperforms the pilot-based estimation. Performance gap is more significant for the smaller packet size due to the number of pilot symbols being insufficient for obtaining a reliable channel estimate. Fig. 5a contains an additional BER curve corresponding to the blind channel estimation using QPSK modulation. The use of QPSK was made possible by artificial correction of the scaling factor ambiguity using simulation genie. Comparison of the QPSK and DEQPSK curves indicates that in the presence of frequency-selective

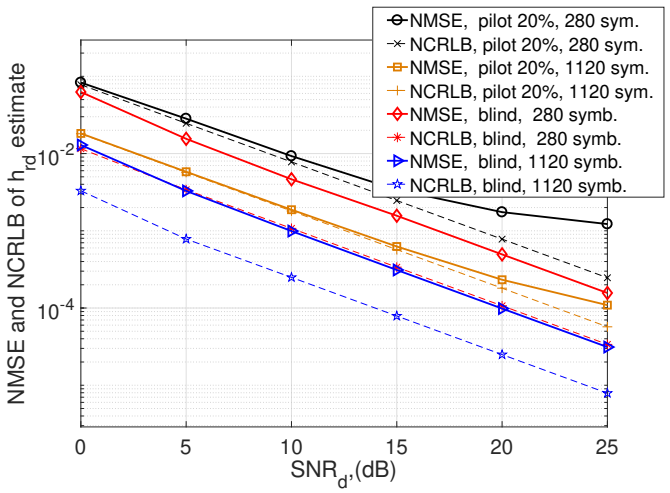

(a)

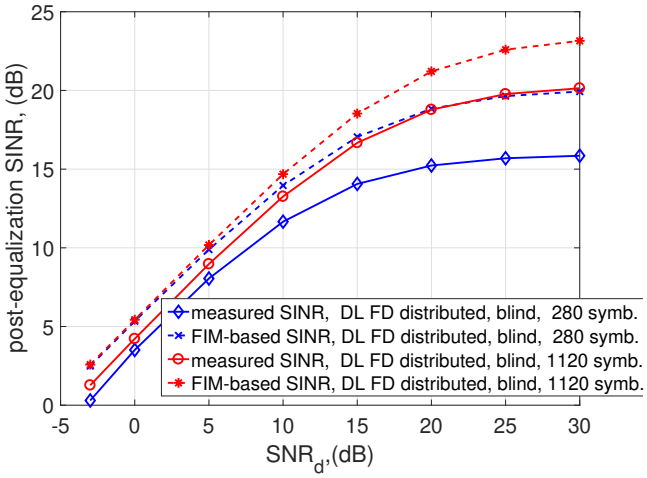

(b)

Fig. 3. FD relay **downlink**: (a) NMSE and NCRLB for channel estimation at the destination; (b) Theoretical upper bound and measured post-equalization SINR; (non-linear SI, SIR=10dB).

fading, the degradation due to the use of DEQPSK is less than 1dB and is mostly present in the low SNR region, where performance is mostly limited by the AWGN.

D. Post-equalization SINR: analytical upper bound vs. measured

The post-equalization SINR plots are provided in Fig. 3b and 4b for DL and UL directions, respectively. The behavior is almost identical in both cases. The plots contain curves based on the analytical expression (21) and provide an upper bound on the achievable post-equalization SINR. The expression

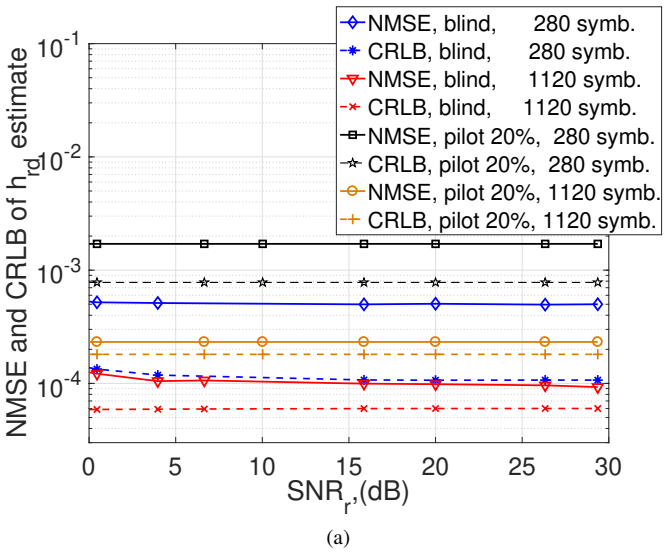

(a)

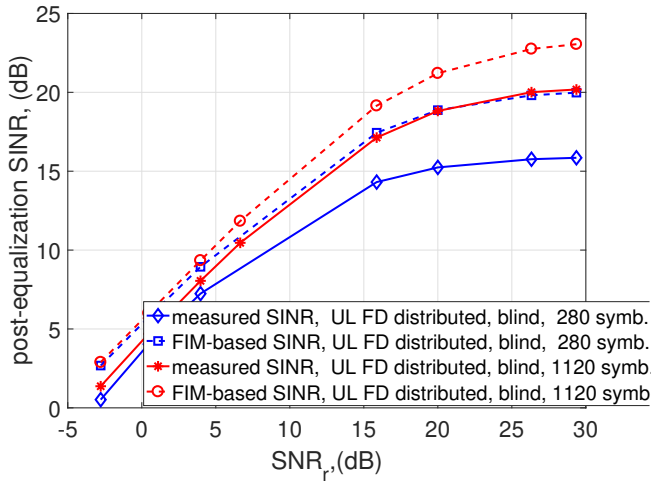

(b)

Fig. 4. FD relay **uplink**: (a) NMSE and NCRLB for channel estimation at the destination; (b) Theoretical upper bound and measured post-equalization SINR; (non-linear SI, SIR=10dB).

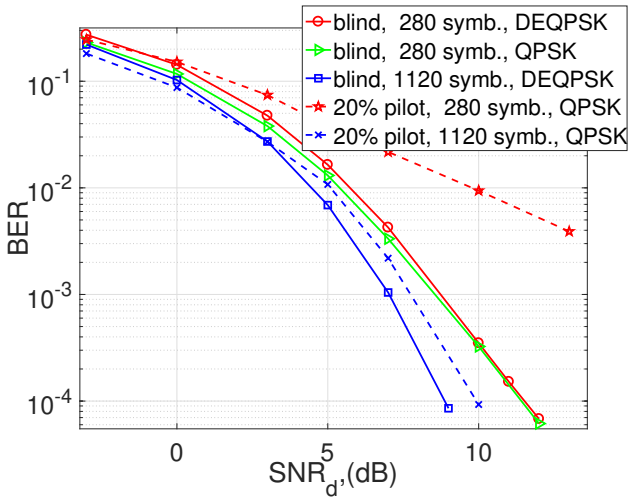

(a)

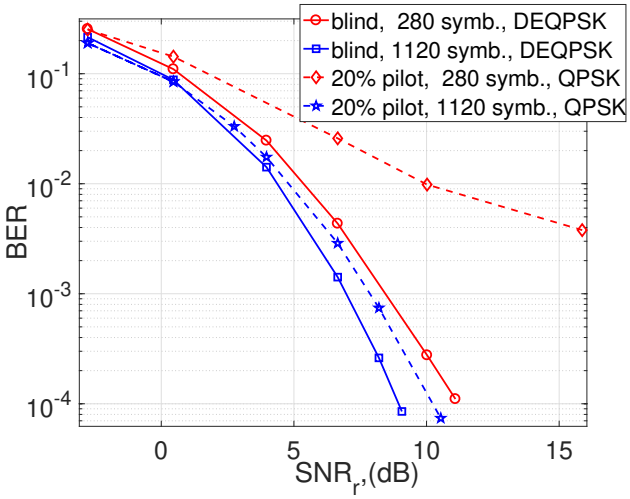

(b)

Fig. 5. BER performance for blind and pilot-based estimation (FD relay with non-linear SI, VGA gain 10dB, SIR=10dB): (a) BER for DL. (b) BER for UL.

(21) incorporating the Fisher Information Matrix for the blind estimation at the destination as well as the aspects of the SI cancellation provides a tighter upper bound than the SINR expression that assumes ideal channel estimation. The added advantage of this expression is that it provides a method of predicting the post-equalization SINR without having to simulate the system and measure the channel estimation error. The accuracy of the prediction depends on the size of the gap between CRLB and the actual channel estimation performance, i.e., NMSE. The plots also contain the SINR measured via simulation and computed using expression (29). The gap between the analytical upper bound and measured SINR is due to the fact that the blind channel estimation method that we use for this evaluation is not able to achieve the CRLB.

E. Spectral efficiency analysis

Fig. 6 contains the plots of the spectral efficiency for DL and UL, respectively. The spectral efficiency value is computed using the post-equalization SINR measured at the destination node and are based on the following expressions:

$$\left(\frac{C}{B}\right)_{\text{FD, blind}} = \log_2\left(1+\text{SINR}_{\text{FD, blind}}\right), \tag{30}$$

$$\left(\frac{C}{B}\right)_{\text{FD, pilot-based}} = (1-\beta)\log_2\left(1+\text{SINR}_{\text{FD, pilot-based}}\right). \tag{31}$$

The parameter of β in (31) represents the pilot allocation ratio, i.e., $\beta = 0.2$ indicates that 20% of the resources are allocated to the pilot symbols in the case of pilot-based channel estimation. The 20% pilot allocation assumption is based on practical communication systems: for example, in GSM, approximately 17% of the bits within the down link time slot are allocated to the training sequence. In the case of 4-Cell-specific Reference Signal port configuration of LTE, approximately 14% of resource elements are allocated to the reference symbols (not counting the additional cyclic prefix overhead). The blind channel estimation results are based on 280 and 1120 samples/estimate. The curves corresponding to

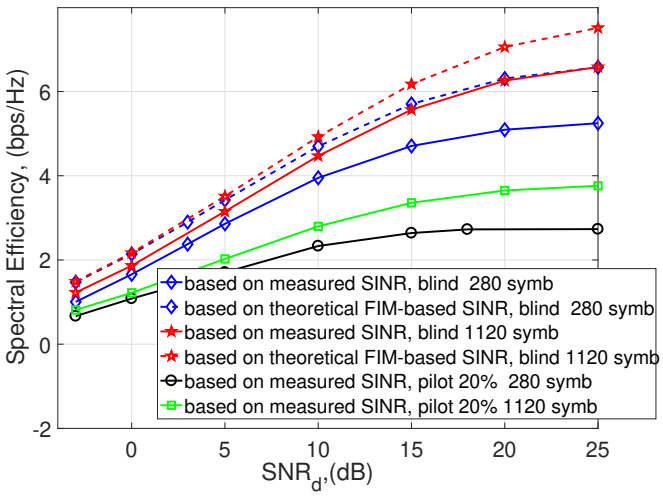

(a)

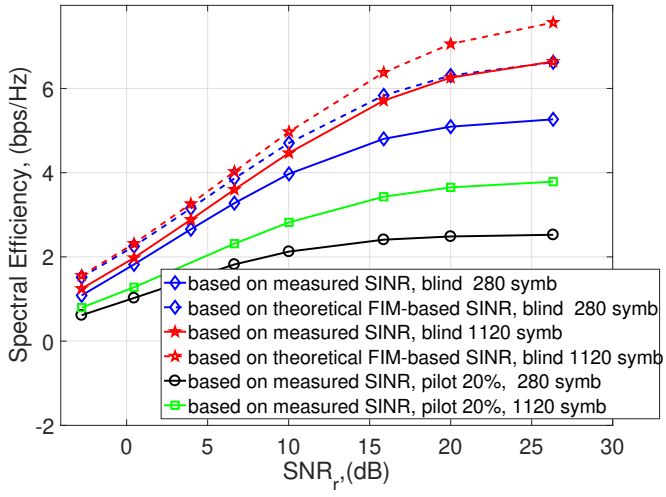

(b)

Fig. 6. Spectral Efficiency of the relay link: (a) downlink; (b) uplink; (non-linear SI, SIR=10dB).

the blind and pilot-based channel estimation are based on the post-equalization SINR measured via simulation. Curves based on the analytical upper bound for post-equalization SINR given in expression (21) show that higher spectral efficiency can be achieved if more optimal blind estimation methods are employed. According to Fig. 6, the blind approach results in superior spectral efficiency relative to the pilot-based method, with the greatest gain at the higher SNR: 2.5 bps/Hz and 2 bps/Hz for the large and small packet sizes, respectively. The spectral efficiency gain is due in part to freed up resources that would otherwise be allocated to the pilot symbols and in part due to better channel estimation performance of the blind approach.

V. Conclusion

In this paper, we studied the feasibility of employing blind channel estimation in the context of two-hop full-duplex relaying. The evaluation was performed for both DL and UL directions as well as for large and small transmission packet sizes. Analytical performance bounds were derived for blind channel estimation and compared with those of a pilot-based approach, where 20% pilot allocation was assumed. Performance metrics such as NMSE and BER were measured via link simulation under frequency-selective fading conditions and compared for the two channel estimation techniques. The spectral efficiency based on the measured post-equalization SINR was also compared. Both analytical and simulated results indicate that blind estimation outperforms the pilot-based approach. The BER performance gain was especially significant for the smaller packet size, where the number of pilot symbols was insufficient for obtaining a reliable estimate. The CRLB expression predicted that blind estimation performance at the destination node is independent of the SINR level at the relay receiver, i.e., noise and self-interference introduced at the relay are as useful for blind estimation as the signal of interest as long as all of these components pass through the same channel. This prediction was confirmed via simulation, where measured channel estimation NMSE was flat across a wide range of SNR levels at the relay receiver.

Furthermore, the analytical expression for post-equalization SINR at the destination node was derived. A modification to this expression was proposed, where the channel estimation error is replaced by the inverse of the Fisher information matrix. Such expression provides an purely analytical upper bound for the post-equalization SINR by eliminating the need for measurement of the channel estimation error. The post-equalization SINR measured via simulation was compared to this analytical bound.

Finally, the computational complexity of the two channel estimation techniques was evaluated and compared. It was found that computational complexity of the second-order-statistic-based blind estimation is independent of the packet size. This is not the case for the pilot-based estimation. Compared to the pilot-based method, blind approach required 20% greater number of FLOPs for small packet size, but 98% fewer FLOPs for the large packet size.

The proposed blind channel estimation approach was found to be a viable option that can be used to further improve the spectral efficiency of a FD relay system. In the future, it would be beneficial to compare the two channel estimation techniques in the context of the full-duplex relay link employing OFDM. In such a system, the channel estimation dynamic is changed due to the use of a cyclic prefix, which significantly impacts the channel characteristics. Additionally, it would be interesting to evaluate situations where the channel identifiability conditions are not perfectly met, i.e., some sub-channels having common or nearly common zeros.

Appendix A
Simplified Equivalent Model of the FD Relay Link

This section shows how we arrive at the simplified equivalent model of the FD relay link that is considered in this paper. The mixed-signal baseband equivalent model is depicted in Fig. 7a. Significantly simplified corresponding discrete-time model is then provided in 7b, where for simplicity, we focus on a single sub-channel configuration (i.e., $L = 1$).

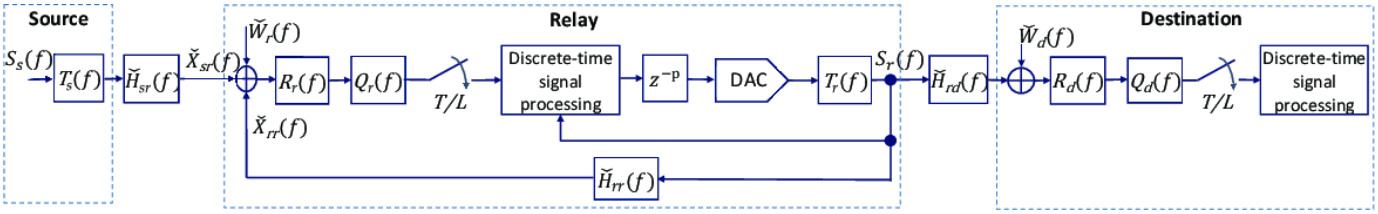

(a) The continuous-time baseband system model

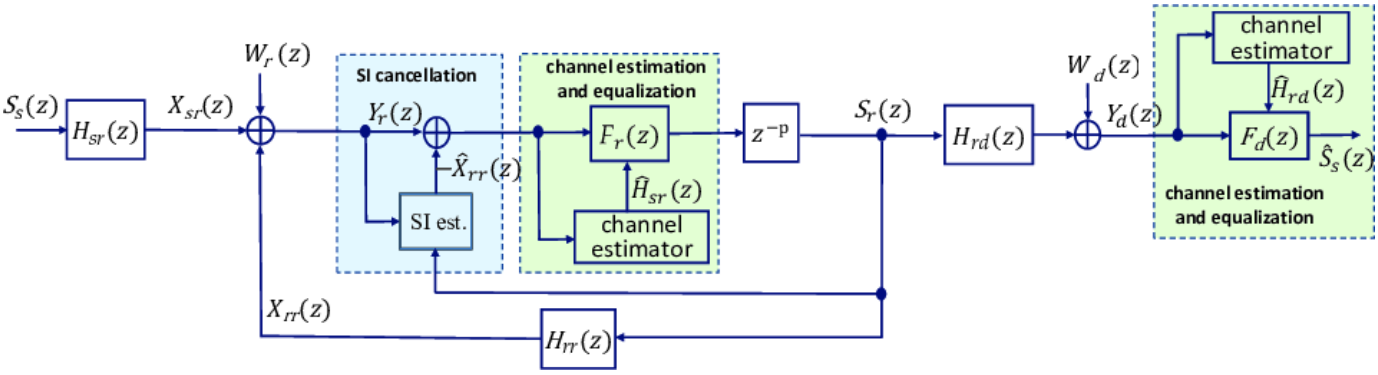

(b) The simplified equivalent model

Fig. 7. Simplification of the discrete-time system model (FD relay link with distributed equalization)

According to Fig. 7b, the signal at the relay receiver is defined as,

$$Y_r(z) = H_{sr}(z)S_s(z) + W_r(z) + H_{rr}(z)S_r(z). \quad (32)$$

Similarly, the signal at the destination receiver is given by,

$$\begin{aligned} Y_d(z) =& Q_d(z)R_d(z)\check{H}_{rd}(z)T_r(z)S_r(z)+Q_d(z)R_d(z)\check{W}_r(z) \\ =& H_{rd}(z)S_r(z) + W_r(z). \end{aligned} \quad (33)$$

The equivalent system model reflecting the simplifications of (32), (33) is shown in Fig. 7b. The signal at the relay output (assuming no SI cancellation):

$$\begin{aligned} S_r(z) \;=\; & F_r(z)H_{sr}(z)S_s(z)z^{-p} \\ & +H_{rr}(z)S_r(z)z^{-p} + F_r(z)W_r(z)z^{-p}. \end{aligned} \quad (34)$$

Next, incorporating the SI cancellation,

$$\begin{aligned} S_r(z) = & F_r(z)H_{sr}(z)S_s(z)z^{-p} + H_{rr}(z)S_r(z)z^{-p} \\ & -\hat{H}_{rr}(z)S_r(z)z^{-p} + F_r(z)W_r(z)z^{-p}. \end{aligned} \quad (35)$$

Rearranging the terms, we obtain IIR formulation,

$$\begin{aligned} S_r(z) \;=\; & \frac{\big[F_r(z)H_{sr}(z)S_s(z) + F_r(z)W_r(z)\big]z^{-p}}{1 - H_{rr}(z)z^{-p} - \hat{H}_{rr}(z)z^{-p}} \\ =\; & \frac{F_r(z)\big[H_{sr}(z)S_s(z) + W_r(z)\big]z^{-p}}{1 - \widetilde{H}_{rr}(z)z^{-p}}, \end{aligned} \quad (36)$$

where $\widetilde{H}_{rr}(z)$ represents the error in SI channel estimation. If this estimation error is sufficiently small, then according to (36), the expression is transformed from IIR to FIR form. Then, according to Fig. 7b, the expression for signal at the destination receiver is

$$Y_d(z) = \frac{H_{rd}(z)\big[H_{sr}(z)S_s(z) + W_r(z)\big]z^{-p}}{1 - \widetilde{H}_{rr}(z)z^{-p}} + W_d(z). \quad (37)$$

APPENDIX B
MMSE EQUALIZER FOR DESTINATION OF FD RELAY, DISTRIBUTED CHANNEL EQUALIZATION

We start by defining the composite source-destination channel as, $\mathbf{H}_{sd;\,n} = \mathbf{H}_{rd;\,n}\mathbf{F}_{r;\,n}\mathbf{H}_{sr;\,n-p}$, and the effective channel from the source of the self-interference at the relay to the destination, $\mathbf{H}_{eff1;\,n} = \mathbf{H}_{rd;\,n}\mathbf{F}_{r;\,n}\widetilde{\mathbf{H}}_{rr;\,n-p}$. The estimated effective and SI channels at time instance n are then $\widehat{\mathbf{H}}_{sd;\,n} = \mathbf{H}_{sd;\,n} + \widetilde{\mathbf{H}}_{sd;\,n}$, $\widehat{\mathbf{H}}_{rr;\,n} = \mathbf{H}_{rr;\,n} + \widetilde{\mathbf{H}}_{rr;\,n}$. Defining the estimation error matrices for effective source-destination and SI channels as $\widetilde{\mathbf{H}}_{sd;\,n}$ and $\widetilde{\mathbf{H}}_{rr;\,n}$, respectively, the signal received at the destination is given by

$$\begin{aligned} \mathbf{y}_{d;\,n} \;=\; & \mathbf{H}_{sd;\,n}\mathbf{s}_{s;\,n-p} + \mathbf{H}_{rd;\,n}\mathbf{F}_{r;\,n}\widetilde{\mathbf{H}}_{rr;\,n}\mathbf{s}_{r;\,n-p} \\ & +\mathbf{H}_{rd;\,n}\mathbf{F}_{r;\,n}\mathbf{w}_{r;\,n-p}+\mathbf{w}_{d;\,n} \\ =\; & \mathbf{H}_{sd;\,n}\mathbf{s}_{s;\,n-p}+\mathbf{w}_{eff1;\,n}, \end{aligned} \quad (38)$$

where

$$\begin{aligned} \mathbf{w}_{eff1;n} \;=\; & \mathbf{H}_{rd;n}\mathbf{F}_{r;n}\widetilde{\mathbf{H}}_{rr;n}\mathbf{s}_{r;\,n-p} \\ & +\mathbf{H}_{rd;\,n}\mathbf{F}_{r;\,n}\mathbf{w}_{r;\,n-p} + \mathbf{w}_{d;\,n}, \end{aligned} \quad (39)$$

and $\mathbf{s}_{r;\,n}$ represents the vector of symbols transmitted by the relay. Hence,

$$\begin{aligned} \mathbf{C}_{y;n} =& \\ & = E\big[(\mathbf{H}_{sd;n}\mathbf{s}_{s;n-p}+\mathbf{w}_{eff1;n})\,(\mathbf{s}^H_{s;n-p}\mathbf{H}^H_{sd;n}+\mathbf{w}^H_{eff1;n})\big] \\ & = \mathbf{H}_{sd;\,n}\mathbf{H}^H_{sd;\,n} + \mathbf{C}_{w_{eff1;\,n}}. \end{aligned} \quad (40)$$

The general expression (40) for the covariance matrix is the same for both end-point and distributed configurations. Next, we focus on the parts that are different.

The effective noise and interference covariance matrix, $\mathbf{C}_{w_{eff1}}$, is defined in (43). Substituting (43) into (40) results in

expression (44). We use the well-known expression for MMSE estimator,

$$\mathbf{F}_{d;\,n} = \mathbf{C}_{sy;\,n}\mathbf{C}_{y;\,n}^{-1}, \tag{41}$$

where assuming that $\mathbf{C}_{s;\,n} = E\left[\mathbf{s}_{s;\,n-p}\mathbf{s}_{s;\,n-p}^{H}\right] = \mathbf{I}$,

$$\begin{aligned}\mathbf{C}_{sy;\,n} &= E(\mathbf{s}_{s;\,n-p}\mathbf{y}_{s;\,n}^{H}) \\ &= E\left[\mathbf{s}_{s;\,n-p}(\mathbf{s}_{s;\,n-p}^{H}\mathbf{H}_{sd;\,n}^{H} + \mathbf{w}_{eff1;\,n}^{H})\right] \\ &= \mathbf{C}_{s;\,n}\mathbf{H}_{sd;\,n}^{H} = \mathbf{H}_{sd;\,n}^{H}. \end{aligned}\tag{42}$$

Substituting (40) and (42) into (41), results in the equalizer expression (45). The channel equalization at the relay produces composite channel $\mathbf{F}_{r;\,n}\mathbf{H}_{sr;\,n-p}$ that is close to all-pass channel not satisfying the identifiability condition for the blind channel estimation method we have chosen. Using the estimated RD channel, $\widehat{\mathbf{H}}_{rd;\,n}$, in (45) instead of $\mathbf{H}_{sd;\,n}$, results in a sufficiently good performance as evident from the simulation results.

APPENDIX C
MMSE EQUALIZER FOR DESTINATION OF FD RELAY, END-POINT CHANNEL EQUALIZATION

According to Fig. 2, the end-point-configuration has no equalizer, $\mathbf{F}_{r;\,n}$, at the relay receiver. Hence, the equivalent channel between the source and destination becomes, $\mathbf{H}_{sd;\,n} = \mathbf{H}_{rd;\,n}\mathbf{H}_{sr;\,n-p}$, and the symbol vector received at the destination becomes,

$$\begin{aligned}\mathbf{y}_{d;\,n} &= \mathbf{H}_{sd;\,n}\mathbf{s}_{s;\,n-p} + \mathbf{H}_{rd;\,n}\widetilde{\mathbf{H}}_{rr;\,n}\mathbf{s}_{r;\,n-p} \\ &\quad + \mathbf{H}_{rd;\,n}\mathbf{w}_{r;\,n-p} + \mathbf{w}_{d;\,n} \\ &= \mathbf{H}_{sd;\,n}\mathbf{s}_{s;\,n-p} + \mathbf{w}_{eff_2;\,n}. \end{aligned}\tag{47}$$

where $\mathbf{s}_{r;\,n}$ represents the vector of symbols transmitted by the relay. Recalling that $\mathbf{C}_{sy;\,n} = \mathbf{H}_{sd;\,n}^{H}$, the equalizer at the destination of end-point configuration is defined as,

$$\begin{aligned}\mathbf{F}_{d;\,n} &= \mathbf{C}_{sy;\,n}\mathbf{C}_{y;\,n}^{-1} \\ &\approx \mathbf{H}_{sd;\,n}^{H}\left(\mathbf{H}_{sd;\,n}\mathbf{H}_{sd;\,n}^{H} + \mathbf{C}_{w_{eff_2};\,n}\right)^{-1}, \end{aligned}\tag{48}$$

where

$$\begin{aligned}\mathbf{C}_{w_{eff_2};n} \approx & \\ &\approx \mathbf{H}_{rd;n}\widetilde{\mathbf{H}}_{rr;n}\mathbf{H}_{sr;n-2p}\mathbf{H}_{sr;n-2p}^{H}\widetilde{\mathbf{H}}_{rr;n}^{H}\mathbf{H}_{sr;n-p}^{H} \\ &\quad + \sigma_{w_r}^2\mathbf{H}_{rd;n}\left(\widetilde{\mathbf{H}}_{rr;n}\widetilde{\mathbf{H}}_{rr;n}^{H} + \mathbf{I}\right)\mathbf{H}_{rd;n}^{H} + \sigma_{w_d}^2\mathbf{I}. \end{aligned}\tag{49}$$

APPENDIX D
POST-EQUALIZATION SINR FOR FD RELAY LINK, DISTRIBUTED EQUALIZATION AND BLIND CHANNEL ESTIMATION:

In this derivation, we incorporate channel estimation error into the definition of the symbol estimation error at the destination. First, the post-equalization symbol error is defined as, $\mathbf{e}_s = \mathbf{s}_{s;\,n} - \mathbf{F}_{d;\,n}\mathbf{y}_{d;\,n} + \widetilde{\mathbf{F}}_{d;\,n}\mathbf{y}_{d;\,n}$, where $\mathbf{F}_{d;\,n}$ is the ideal equalizer matrix, and $\widetilde{\mathbf{F}}_{d;\,n} = \widetilde{\mathbf{C}}_{sy;\,n}\mathbf{C}_{y;\,n}^{-1} = \widetilde{\mathbf{H}}_{rd;\,n}^{H}\mathbf{C}_{y;\,n}^{-1}$.

Variance of $\mathbf{e}_s$ is provided in (50), where the approximation of the channel estimation error covariance matrix $\widetilde{\mathbf{H}}_{rd;\,n}\widetilde{\mathbf{H}}_{rd;\,n}^{H}$ by the Fisher Information Matrix $\mathbf{J}(\hat{\mathbf{h}}_{rd;\,n})$ results in expression representing the lower bound on the symbol estimation error variance. The advantage of this approach is that it provides purely analytical expression and doesn't need to rely on the simulation to determine the channel estimation error covariance matrix. This results in expression (51) for the upper bound on the post-equalization SINR, where the covariance matrix, $\mathbf{C}_{y;\,n}$, is defined in (52). In the final step of (52), it was assumed that the term $\mathbf{H}_{eff_3;\,n}\mathbf{F}_{r;\,n-p}\widetilde{\mathbf{H}}_{rr;\,n-p}\mathbf{C}_{s_r;\,n-2p}\widetilde{\mathbf{H}}_{rr;\,n-p}^{H}\mathbf{F}_{r;\,n-p}^{H}\mathbf{H}_{eff_3;\,n}^{H}$ is sufficiently small to be neglected.

APPENDIX E
CRLB FOR BLIND ESTIMATION OF EFFECTIVE CHANNEL AT THE DESTINATION

The following derivation is applicable to both *end-point* and *distributed* configurations, with system equations given by (47) and (38), respectively. In both cases, $\mathbf{y}_{d;\,n} \sim \mathcal{CN}(\mathbf{H}_{sd;\,n}\mathbf{s}_{s;\,n-p}, \mathbf{C}_{w_{eff};\,n})$, defined in (53), where $\theta_n = \begin{bmatrix}\mathbf{s}_{s;\,n}^{T} & \mathbf{h}_{sd;\,n}^{T}\end{bmatrix}^{T}$, is $[(A+M+1)\times 1]$ joint parameter of interest vector. The noise and interference covariance matrix, $\mathbf{C}_{w_{eff};\,n}$, for distributed configuration is given by (43). Also, the effective channel $\mathbf{H}_{sd;\,n}$, between the source and destination is defined as $\mathbf{H}_{sd;\,n} = \mathbf{H}_{rd;\,n}\mathbf{F}_{r;\,n}\mathbf{H}_{sr;\,n-p}$. The Fisher Information Matrix (FIM) is given by

$$\mathbf{J}(\theta) = E\left[\left(\frac{\partial \ln p(\mathbf{y}_{d;\,n};\theta)}{\partial \theta^{*}}\right)\left(\frac{\partial \ln p(\mathbf{y}_{d;\,n};\theta)}{\partial \theta^{*}}\right)^{H}\right], \tag{58}$$

and according to [11], the elements of $\mathbf{J}(\theta)$ are defined in (54), where in our case, $\mu_y = \mathbf{S}_{s;\,n}\mathbf{h}_{sd;\,n}$, and the last two terms are zeros. According to (3)-(4), the expension of the term $\mathbf{S}_{s;\,n}\mathbf{h}_{sd;\,n}$ is given by (55). Hence,

$$\frac{\partial \mathbf{S}_{s;\,n}\mathbf{h}_{sd}}{\partial \theta_n[i]} = \begin{cases} \mathbf{h}_{sd}^{(i)}, & \text{if } 0 \le i < A \\ \mathbf{s}_{s}^{(i-A)}, & \text{if } A \le i \le A+M \end{cases} \tag{59}$$

and $\frac{\partial \mathbf{S}_{s;\,n}\mathbf{h}}{\partial \theta_n} = \begin{bmatrix}\mathbf{H}_{sd;\,n} & \mathbf{S}_{s;\,n}\end{bmatrix}$. Hence,

$$\begin{aligned}\mathbf{J}(\theta_n) &= \begin{bmatrix}\mathbf{H}_{sd;\,n}^{H} \\ \mathbf{S}_{s;\,n}^{H}\end{bmatrix}\mathbf{C}_{w_{eff};\,n}^{-1}\begin{bmatrix}\mathbf{H}_{sd;\,n} & \mathbf{S}_{s;\,n}\end{bmatrix} \\ &= \begin{bmatrix}\mathbf{H}_{sd;\,n}^{H}\mathbf{C}_{w_{eff};\,n}^{-1}\mathbf{H}_{sd;\,n} & \mathbf{H}_{sd;\,n}^{H}\mathbf{C}_{w_{eff};\,n}^{-1}\mathbf{S}_{s;\,n} \\ \mathbf{S}_{s;\,n}^{H}\mathbf{C}_{w_{eff};\,n}^{-1}\mathbf{H}_{sd;\,n} & \mathbf{S}_{s;\,n}^{H}\mathbf{C}_{w_{eff};\,n}^{-1}\mathbf{S}_{s;\,n}\end{bmatrix}, \end{aligned}$$

and

$$\mathrm{CRLB}(\theta_n) = \mathbf{J}^{-1}(\theta_n) = \begin{bmatrix}\mathbf{B}_{11} & \mathbf{B}_{12} \\ \mathbf{B}_{21} & \mathbf{B}_{22}\end{bmatrix}, \tag{60}$$

where $\mathbf{B}_{22}$ is the partition of the joint CRLB matrix corresponding to the $\mathrm{CRLB}(\mathbf{h})$, which can be computed using (56), which is based on *partitioned matrix inversion lemma*. If instead of $\mathbf{h}_{sd}$, the estimation of $\mathbf{h}_{rd}$ at the destination is of interest, then expression (56) turns into (57), where $\mathbf{S}_{r;\,n}$ represents the signal transmitted by the relay,

$$\mathbf{S}_{r;n} = \mathbf{F}_{r;\,n}\mathbf{H}_{sr;\,n}\mathbf{S}_{s;n} + \mathbf{F}_{r;\,n}\widetilde{\mathbf{H}}_{rr;\,n}\mathbf{S}_{r;\,n-p} + \mathbf{F}_{r;\,n}\mathbf{w}_{r;\,n}, \tag{61}$$

and $\mathbf{C}_{w_{eff}} = \sigma_{w_d}^2\mathbf{I}$. In (61), the noise and residual SI at the relay are included in the signal transmitted by the relay and are not part of the noise covariance matrix. Because these signals pass through the RD channel, they carry information about this channel.

$$\begin{aligned}\mathbf{C}_{w_{eff1}} &= E\left[\mathbf{w}_{eff1;\,n}\mathbf{w}_{eff1;\,n}^H\right] = \mathbf{H}_{eff1;\,n}\mathbf{F}_{r;\,n-p}\mathbf{H}_{sr;\,n-2p}\mathbf{H}_{sr;\,n-2p}^H\mathbf{F}_{r;\,n-p}^H\mathbf{H}_{eff1;\,n}^H\\ &\quad+\mathbf{H}_{eff1;\,n}\mathbf{F}_{r;\,n-p}\widetilde{\mathbf{H}}_{rr;\,n-p}\mathbf{R}_{s_r;\,n-2p}\widetilde{\mathbf{H}}_{rr;\,n-p}^H\mathbf{F}_{r;\,n-p}^H\mathbf{H}_{eff1;\,n}^H\\ &\quad+\sigma_{w_r}^2\left(\mathbf{H}_{eff1;\,n}\mathbf{F}_{r;\,n-p}\mathbf{F}_{r;\,n-p}^H\mathbf{H}_{eff1;\,n}^H+\mathbf{H}_{rd;\,n}\mathbf{F}_{r;\,n}\mathbf{F}_{r;\,n}^H\mathbf{H}_{rd;\,n}^H\right)+\sigma_{w_d}^2\mathbf{I}\\ &\approx \mathbf{H}_{eff1;\,n}\mathbf{F}_{r;\,n-p}\mathbf{H}_{sr;\,n-2p}\mathbf{H}_{sr;\,n-2p}^H\mathbf{F}_{r;\,n-p}^H\mathbf{H}_{eff1;\,n}^H\\ &\quad+\sigma_{w_r}^2\mathbf{H}_{rd;\,n}\mathbf{F}_{r;\,n}\left(\widetilde{\mathbf{H}}_{rr;\,n}\widetilde{\mathbf{H}}_{rr;\,n}^H+\mathbf{I}\right)\mathbf{F}_{r;\,n}^H\mathbf{H}_{rd;\,n}^H+\sigma_{w_d}^2\mathbf{I}. \end{aligned}\tag{43}$$

$$\begin{aligned}\mathbf{C}_{y;\,n} &\approx \mathbf{H}_{sd;\,n}\mathbf{H}_{sd;\,n}^H+\mathbf{H}_{eff1;\,n}\mathbf{F}_{r;\,n-p}\mathbf{H}_{sr;\,n-2p}\mathbf{H}_{sr;\,n-2p}^H\mathbf{F}_{r;\,n-p}^H\mathbf{H}_{eff1;\,n}^H\\ &\quad+\sigma_{w_r}^2\mathbf{H}_{rd;\,n}\mathbf{F}_{r;\,n}\left(\widetilde{\mathbf{H}}_{rr;\,n}\widetilde{\mathbf{H}}_{rr;\,n}^H+\mathbf{I}\right)\mathbf{F}_{r;\,n}^H\mathbf{H}_{rd;\,n}^H+\sigma_{w_d}^2\mathbf{I}. \end{aligned}\tag{44}$$

$$\begin{aligned}\mathbf{F}_{d;\,n} &= \mathbf{C}_{sy;\,n}\mathbf{C}_{y;\,n}^{-1}=\mathbf{H}_{sd;\,n}^H\mathbf{C}_{y;\,n}^{-1}\approx\mathbf{H}_{rd;\,n}^H\mathbf{C}_{y;\,n}^{-1}\\ &= \mathbf{H}_{rd;\,n}^H\left(\mathbf{H}_{sd;\,n}\mathbf{H}_{sd;\,n}^H+\mathbf{C}_{w_{eff1}}\right)^{-1}\approx\mathbf{H}_{rd;\,n}^H\left(\mathbf{H}_{rd;\,n}\mathbf{H}_{rd;\,n}^H+\mathbf{C}_{w_{eff1}}\right)^{-1}. \end{aligned}\tag{45}$$

$$\begin{aligned}\mathbf{C}_{w_{eff1}} &\approx \mathbf{H}_{eff1;\,n}\mathbf{F}_{r;\,n-p}\mathbf{H}_{sr;\,n-2p}\mathbf{H}_{sr;\,n-2p}^H\mathbf{F}_{r;\,n-p}^H\mathbf{H}_{eff1;\,n}^H\\ &\quad+\frac{1}{\mathrm{SNR}_r}\mathbf{H}_{rd;\,n}\mathbf{F}_{r;\,n}\left(\widetilde{\mathbf{H}}_{rr;\,n}\widetilde{\mathbf{H}}_{rr;\,n}^H+\mathbf{I}\right)\mathbf{F}_{r;\,n}^H\mathbf{H}_{rd;\,n}^H+\frac{1}{\mathrm{SNR}_d}\mathbf{I}\Big)^{-1}. \end{aligned}\tag{46}$$

$$\begin{aligned}\sigma_e^2 &= \frac{1}{N}\mathrm{tr}\left\{E\left[(\mathbf{s}_{s;\,n}-\mathbf{F}_{d;\,n}\mathbf{y}_{d;\,n}+\widetilde{\mathbf{F}}_{d;\,n}\mathbf{y}_{d;\,n})(\mathbf{s}_{s;\,n}-\mathbf{F}_{d;\,n}\mathbf{y}_{d;\,n}+\widetilde{\mathbf{F}}_{d;\,n}\mathbf{y}_{d;\,n})^H\right]\right\}\\ &= 1+\frac{1}{N}\mathrm{tr}\left\{\widetilde{\mathbf{H}}_{rd;\,n}\widetilde{\mathbf{H}}_{rd;\,n}^H\mathbf{C}_{y;\,n}^{-1}\right\}-\frac{1}{N}\mathrm{tr}\left\{\mathbf{H}_{rd;\,n}\mathbf{H}_{rd;\,n}^H\mathbf{C}_{y;\,n}^{-1}\right\}\\ &\geq 1+\frac{1}{N}\mathrm{tr}\left\{\mathbf{J}^{-1}(\mathbf{h}_{rd;\,n})\mathbf{C}_{y;\,n}^{-1}\right\}-\frac{1}{N}\mathrm{tr}\left\{\mathbf{H}_{rd;\,n}\mathbf{H}_{rd;\,n}^H\mathbf{C}_{y;\,n}^{-1}\right\}, \end{aligned}\tag{50}$$

$$\mathrm{SINR}_{distributed} = \frac{1}{\sigma_e^2}-1\leq\frac{1}{1+\frac{1}{N}\mathrm{tr}\left\{\mathbf{J}^{-1}(\mathbf{h}_{rd;\,n})\mathbf{C}_{y;\,n}^{-1}\right\}-\frac{1}{N}\mathrm{tr}\left\{\mathbf{H}_{rd;\,n}\mathbf{H}_{rd;\,n}^H\mathbf{C}_{y;\,n}^{-1}\right\}}-1,\tag{51}$$

$$\begin{aligned}\mathbf{C}_{y;\,n} &= \mathbf{H}_{sd;\,n}\mathbf{H}_{sd;\,n}^H+\mathbf{H}_{sd;\,n}\mathbf{F}_{r,n-p}\mathbf{H}_{sr;\,n-2p}\mathbf{H}_{sr;\,n-2p}^H\mathbf{F}_{r;\,n-p}^H\mathbf{H}_{eff_3;\,n}^H\\ &\quad+\mathbf{H}_{eff_3;\,n}\mathbf{F}_{r;\,n-p}\widetilde{\mathbf{H}}_{rr;\,n-p}\mathbf{R}_{s_r;\,n-2p}\widetilde{\mathbf{H}}_{rr;\,n-p}^H\mathbf{F}_{r;\,n-p}^H\mathbf{H}_{eff_3;\,n}^H\\ &\quad+\frac{1}{\mathrm{SNR}_r}\left(\mathbf{H}_{eff_3;\,n}\mathbf{F}_{r;\,n-p}\mathbf{F}_{r;\,n-p}^H\mathbf{H}_{eff_3;\,n}^H+\mathbf{H}_{rd;\,n}\mathbf{F}_{r;\,n}\mathbf{F}_{r;\,n}^H\mathbf{H}_{rd;\,n}^H\right)+\frac{1}{\mathrm{SNR}_d}\mathbf{I}\\ &\approx \mathbf{H}_{sd;\,n}\mathbf{H}_{sd;\,n}^H+\mathbf{H}_{eff_3;\,n}\mathbf{F}_{r;\,n-p}\mathbf{H}_{sr;\,n-2p}\mathbf{H}_{sr;\,n-2p}^H\mathbf{F}_{r;\,n-p}^H\mathbf{H}_{eff_3;\,n}^H\\ &\quad+\frac{1}{\mathrm{SNR}_r}\left(\mathbf{H}_{eff_3;\,n}\mathbf{F}_{r;\,n-p}\mathbf{F}_{r;\,n-p}^H\mathbf{H}_{eff_3;\,n}^H+\mathbf{H}_{rd;\,n}\mathbf{F}_{r;\,n}\mathbf{F}_{r;\,n}^H\mathbf{H}_{rd;\,n}^H\right)+\frac{1}{\mathrm{SNR}_d}\mathbf{I}. \end{aligned}\tag{52}$$

ACKNOWLEDGMENT

The authors would like to thank Md Atiqul Islam for sharing his insights into modeling of the non-linear effects present at the FD transceiver. He is currently a Ph.D. student a the department of Electrical and Computer Engineering of the University of Illinois at Chicago.

Konstantin Muranov is a doctoral student in the Department of Electrical and Computer Engineering at the University of Illinois at Chicago. His research interests include wireless communication systems, signal processing, wireless relaying, blind channel estimation, and full-duplex transceivers. Konstantin has been working in the wireless industry since 1999, including such companies as Motorola Mobility and Intel. Over the years, he took part in the development of wireless devices involving 3G, 4G, and 5G technologies. Konstantin received M.S. degree in electrical engineering from the University of Toledo in 1999. He received B.S. degree in electrical engineering from the University of Toledo in 1997.

$$f(\mathbf{y}_{d;\,n};\theta_n) = \frac{1}{\pi^N \det\left[\mathbf{C}_{w_{eff};\,n}\right]} \exp\left\{-(\mathbf{y}_{d;\,n}-\mathbf{H}_{sd;\,n}\mathbf{s}_{s;\,n-p})^H \mathbf{C}^{-1}_{w_{eff};\,n}(\mathbf{y}_{d;\,n}-\mathbf{H}_{sd;\,n}\mathbf{s}_{s;\,n-p})\right\} \tag{53}$$

$$\begin{aligned}[\mathbf{J}(\theta_n)]_{i,j} &= \left(\frac{\partial \mu_y}{\partial \theta_n[i]}\right)^H \mathbf{C}^{-1}_{w_{eff};\,n}\frac{\partial \mu_y}{\partial \theta_n[j]} + \left(\frac{\partial \mu_y}{\partial \theta^*_n[j]}\right)^H \mathbf{C}^{-1}_{w_{eff};\,n}\frac{\partial \mu_y}{\partial \theta^*_n[i]} \\ &\quad + tr\left(\frac{\partial \mathbf{C}_{w_{eff};\,n}}{\partial \theta^*_n}\mathbf{C}^{-1}_{w_{eff};\,n}\frac{\partial \mathbf{C}_{w_{eff};\,n}}{\partial \theta_n}\mathbf{C}^{-1}_{w_{eff};\,n}\right)\end{aligned} \tag{54}$$

$$\mathbf{S}_{s;\,n}\mathbf{h}_{sd;\,n} = \begin{bmatrix} s_s[n]h_{sd}[0] \\ s_s[n+1]h_{sd}[0] + s_s[n]h_{sd}[1] \\ s_s[n+2]h_{sd}[0] + s_s[n+1]h_{sd}[1] + s_s[n]h_{sd}[2] \\ \vdots \\ s_s[n+A-1]h_{sd}[0] + s_s[n+A-2]h_{sd}[1] + ... + s_s[n+A-M-1]h_{sd}[M] \end{bmatrix} \tag{55}$$

$$\text{CRLB}(\mathbf{h}_{sd;\,n}) = \mathbf{B}_{22} = \left[\mathbf{S}^H_{s;\,n}\left(\mathbf{C}^{-1}_{w_{eff}} - \mathbf{C}^{-1}_{w_{eff}}\mathbf{H}_{sd;\,n}\left(\mathbf{H}^H_{sd;\,n}\mathbf{C}^{-1}_{w_{eff}}\mathbf{H}_{sd;\,n}\right)^{-1}\mathbf{H}^H_{sd;\,n}\mathbf{C}^{-1}_{w_{eff}}\right)\mathbf{S}_{s;\,n}\right]^{-1} \tag{56}$$

$$\text{CRLB}(\mathbf{h}_{rd;\,n}) = \left[\mathbf{S}^H_{r;\,n}\left(\mathbf{C}^{-1}_{w_{eff}} - \mathbf{C}^{-1}_{w_{eff}}\mathbf{H}_{rd;\,n}\left(\mathbf{H}^H_{rd;\,n}\mathbf{C}^{-1}_{w_{eff}}\mathbf{H}_{rd;\,n}\right)^{-1}\mathbf{H}^H_{rd;\,n}\mathbf{C}^{-1}_{w_{eff}}\right)\mathbf{S}_{r;\,n}\right]^{-1} \tag{57}$$

Besma Smida (Senior Member, IEEE) is an Associate Professor of Electrical and Computer Engineering with the University of Illinois at Chicago. After completing her appointment as a Post-Doctoral Researcher and later a Lecturer at Harvard University, she became an Assistant Professor of electrical and computer engineering with Purdue University Northwest. She received the M.Sc. and Ph.D. degrees from the University of Quebec (INRS), Montreal, QC, Canada. She was a Research Engineer with the Technology Evolution and Standards Group of Microcell, Inc., (now Rogers Wireless), Montreal. She took part in wireless normalization committees (3GPP, T1P1).

She has served as the Chair for IEEE Women in Engineering, Chicago Section, from 2011 to 2013, and has been the Chair of IEEE Communication Chapter, Chicago Section, since 2019. She currently serves as Editor for the IEEE TRANSACTIONS ON WIRELESS COMMUNICATIONS, Editor of the IEEE OPEN JOURNAL OF THE COMMUNICATIONS SOCIETY, and a Guest Editor SENSORS OPEN ACCESS JOURNAL. Previously she served as an Associate Editor for the IEEE COMMUNICATION LETTERS, and a Guest Editor for special issues of the IEEE JOURNAL ON SELECTED AREAS IN COMMUNICATIONS.

She is a Communication Society Distinguished Lecturer for 2021-2022. She was awarded the INSIGHT Into Diversity Magazine's 2015 "100 Inspiring Women in STEM". She received the Academic Gold Medal of the Governor General of Canada in 2007 and the NSF CAREER award in 2015. Her research focuses on In-band Full-Duplex systems and applications, backscatter modulation, IoT, and two-way communication networks.

Natasha Devroye is a Professor in the Department of Electrical and Computer Engineering at the University of Illinois at Chicago (UIC), which she joined in January 2009. From July 2007 until July 2008 she was a Lecturer at Harvard University. Dr. Devroye obtained her Ph.D in Engineering Sciences from the School of Engineering and Applied Sciences at Harvard University in 2007, and an Honors B. Eng in Electrical Engineering from McGill University in 2001. Dr. Devroye was a recipient of an NSF CAREER award in 2011 and was named UIC's Researcher of the Year in the "Rising Star" category in 2012. She has been an Associate Editor for IEEE Transactions on Wireless Communications, IEEE Journal of Selected Areas in Communications, the IEEE Transactions on Cognitive Communications and Networking and the IEEE Transactions on Information Theory. She co-chaired the Women in Information Theory Society from 2015-2018 and is an Information Theory Society Distinguished Lecturer for 2019-2021. Her research focuses on multi-user information theory and applications to cognitive and software-defined radio, radar, relay, zero-error and two-way communication networks.

REFERENCES

[1] E. Ahmed, A. M. Eltawil, and A. Sabharwal, "Self-interference cancellation with nonlinear distortion suppression for full-duplex systems," *2013 Asilomar Conference on Signals, Systems and Computers*, pp. 1199–1203, Nov 2013.

[2] C. R. Anderson, S. Krishnamoorthy, C. G. Ranson, T. J. Lemon, W. G. Newhall, T. Kummetz, and J. H. Reed, "Antenna isolation, wideband multipath propagation measurements, and interference mitigation for on-frequency repeaters," in *IEEE SoutheastCon, 2004. Proceedings.*, March 2004, pp. 110–114.

[3] P. Arbenz, "Lecture notes on solving large scale eigenvalue problems," *Available online at the following link: https://people.inf.ethz.ch/arbenz/ewp/Lnotes/lsevp.pdf*, 2016.

[4] M. Duarte and A. Sabharwal, "Full-duplex wireless communications using off-the-shelf radios: Feasibility and first results," in *2010 Conference Record of the Forty Fourth Asilomar Conference on Signals, Systems and Computers*, Nov 2010, pp. 1558–1562.

[5] E. Everett, M. Duarte, C. Dick, and A. Sabharwal, "Empowering full-duplex wireless communication by exploiting directional diversity," in *2011 Conference Record of the Forty Fifth Asilomar Conference on Signals, Systems and Computers (ASILOMAR)*, Nov 2011, pp. 2002–2006.

[6] G. B. Giannakis and S. D. Halford, "Blind fractionally spaced equalization of noisy fir channels: direct and adaptive solutions," *IEEE Transactions on Signal Processing*, vol. 45, no. 9, pp. 2277–2292, Sep. 1997.

[7] H. Hamazumi, K. Imamura, N. Iai, K. Shibuya, and M. Sasaki, "A study of a loop interference canceller for the relay stations in an sfn for digital terrestrial broadcasting," in *Global Telecommunications Conference, 2000. GLOBECOM '00. IEEE*, vol. 1, 2000, pp. 167–171 vol.1.

[8] M. Heino, D. Korpi, T. Huusari, E. Antonio-Rodriguez, S. Venkatasubramanian, T. Riihonen, L. Anttila, C. Icheln, K. Haneda, R. Wichman, and M. Valkama, "Recent advances in antenna design and interference cancellation algorithms for in-band full duplex relays," *IEEE Communications Magazine*, vol. 53, no. 5, pp. 91–101, May 2015.

[9] R. Hunger, "Floating point operations in matrix-vector calculus," *Technical Report, version 1.3, Available online at the following link: https://mediatum.ub.tum.de/doc/625604/625604*, 2007.

[10] M. A. Islam and B. Smida, "A comprehensive self-interference model for single-antenna full-duplex communication systems," in *ICC 2019 - 2019 IEEE International Conference on Communications (ICC)*, 2019, pp. 1–7.

[11] S. Kay, *Fundamentals of statistical signal processing: estimation theory*. Prentice Hall, 1993.

[12] S. Khaledian, F. Farzami, B. Smida, and D. Erricolo, "Inherent self-interference cancellation for in-band full-duplex single-antenna systems," *IEEE Transactions on Microwave Theory and Techniques*, vol. 66, no. 6, pp. 2842–2850, 2018.

[13] A. Koohian, H. Mehrpouyan, M. Ahmadian, and M. Azarbad, "Bandwidth efficient channel estimation for full duplex communication systems," in *2015 IEEE International Conference on Communications (ICC)*, June 2015, pp. 4710–4714.

[14] D. Korpi, L. Anttila, V. Syrj¨al¨a, and M. Valkamal, "Widely linear digital self-interference cancellation in direct-conversion full-duplex transceiver," *IEEE Journal on Selected Areas in Communications*, p. 1674–1687, 2014.

[15] D. Korpi, J. Tamminen, M. Turunen, T. Huusari, Y. S. Choi, L. Anttila, S. Talwar, and M. Valkama, "Full-duplex mobile device: pushing the limits," *IEEE Communications Magazine*, vol. 54, no. 9, pp. 80–87, September 2016.

[16] J. H. Lee, "Self-interference cancellation using phase rotation in full-duplex wireless," *IEEE Transactions on Vehicular Technology*, vol. 62, no. 9, pp. 4421–4429, Nov 2013.

[17] P. Lioliou, M. Viberg, M. Coldrey, and F. Athley, "Self-interference suppression in full-duplex mimo relays," in *2010 Conference Record of the Forty Fourth Asilomar Conference on Signals, Systems and Computers*, Nov 2010, pp. 658–662.

[18] E. Moulines, P. Duhamel, J. F. Cardoso, and S. Mayrargue, "Subspace methods for the blind identification of multichannel fir filters," *IEEE Transactions on Signal Processing*, vol. 43, no. 2, pp. 516–525, Feb 1995.

[19] K. Muranov, B. Smida, and N. Devroye, "On channel equalization for full-duplex relay networks," in *2017 IEEE International Conference on Communications (ICC)*, May 2017, pp. 1–6.

[20] K. M. Nasr, J. P. Cosmas, M. Bard, and J. Gledhill, "Performance of an echo canceller and channel estimator for on-channel repeaters in dvb-t/h networks," *IEEE Transactions on Broadcasting*, vol. 53, no. 3, pp. 609–618, Sept 2007.

[21] T. Riihonen, S. Werner, and R. Wichman, "Comparison of full-duplex and half-duplex modes with a fixed amplify-and-forward relay," in *2009 IEEE Wireless Communications and Networking Conference*, April 2009, pp. 1–5.

[22] ——, "Mitigation of loopback self-interference in full-duplex mimo relays," *IEEE Transactions on Signal Processing*, vol. 59, no. 12, pp. 5983–5993, Dec 2011.

[23] T. Riihonen, S. Werner, R. Wichman, and E. Z. B., "On the feasibility of full-duplex relaying in the presence of loop interference," in *2009 IEEE 10th Workshop on Signal Processing Advances in Wireless Communications*, June 2009, pp. 275–279.

[24] T. Riihonen, S. Werner, and R. Wichman, "Residual self-interference in full-duplex mimo relays after null-space projection and cancellation," *2010 Conference Record of the Forty Fourth Asilomar Conference on Signals, Systems and Computers*, 2010.

[25] ——, "Mitigation of loopback self-interference in full-duplex mimo relays," *IEEE Transactions on Signal Processing*, 2011.

[26] W. T. Slingsby and J. P. McGeehan, "Antenna isolation measurements for on-frequency radio repeaters," in *Antennas and Propagation, 1995., Ninth International Conference on (Conf. Publ. No. 407)*, Apr 1995, pp. 239–243 vol.1.

[27] Z. Ting, W. Fang, X. Jing, and J. Lilleberg, "Soft symbol estimation and forward scheme for cooperative relaying," in *2009 IEEE 20th International Symposium on Personal, Indoor and Mobile Radio Communications*, Sept 2009, pp. 3069–3073.

[28] L. Tong, G. Xu, B. Hassibi, and T. Kailath, "Blind channel identification based on second-order statistics: a frequency-domain approach," *IEEE Transactions on Information Theory*, vol. 41, no. 1, pp. 329–334, Jan 1995.

[29] L. Tong, G. Xu, and T. Kailath, "Blind identification and equalization based on second-order statistics: a time domain approach," *IEEE Transactions on Information Theory*, vol. 40, no. 2, pp. 340–349, March 1994.

[30] Y. Tong, *The Multivariate Normal Distribution*. Springer New York, 1990.

[31] D. Tse and P. Viswanath, *Fundamentals of Wireless Communication*. Cambridge University Press, 2005, 2005.

[32] H. H. Zeng and L. Tong, "Blind channel estimation using the second-order statistics: algorithms," *IEEE Transactions on Signal Processing*, vol. 45, no. 8, pp. 1919–1930, Aug 1997.

[33] Z. Zhang, Y. Shen, S. Shao, W. Pan, and Y. Tang, "Full duplex 2×2 mimo radios," in *2014 Sixth International Conference on Wireless Communications and Signal Processing (WCSP)*, Oct 2014, pp. 1–6.

[34] Zhi Ding and Y. Li, "On channel identification based on second-order cyclic spectra," *IEEE Transactions on Signal Processing*, vol. 42, no. 5, pp. 1260–1264, May 1994.